DELFT UNIVERSITY OF TECHNOLOGY

REPORT 09-06

Smoothness-Increasing Convergence-Conserving Spline Filters Applied to Streamline Visualisation of DG Approximations

P. van Slingerland, J.K. Ryan, and C. Vuik

ISSN 1389-6520

Reports of the Department of Applied Mathematical Analysis

Delft 2009

Smoothness-Increasing Convergence-Conserving

Spline Filters

Applied to Streamline Visualisation of DG Approximations

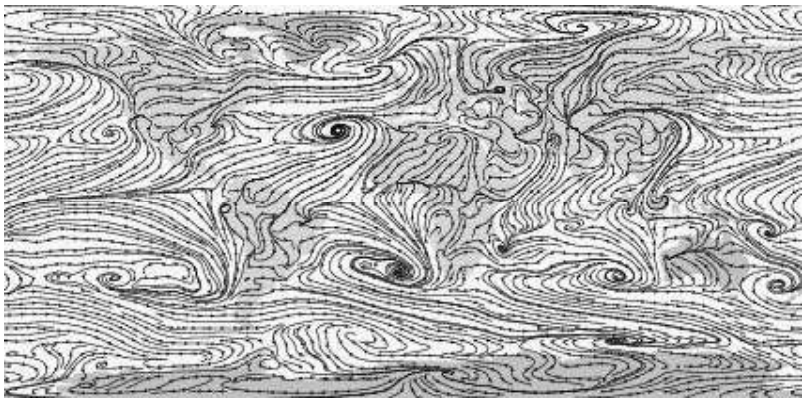

Literature Study

by

Paulien van Slingerland

June 2, 2009

Supervisors:
Prof.dr.ir. C. Vuik
Dr. J.K. Ryan

TU Delft

Contents

1 Introduction **1**

2 Defining the problem **3**
2.1 Introduction . . . 3
2.2 Hyperbolic systems . . . 3
2.3 Discontinuous Galerkin method . . . 4
2.4 Visualisation of the results as streamlines . . . 8
2.5 Conclusion . . . 10

3 Increasing the smoothness **11**
3.1 Introduction . . . 11
3.2 B-splines . . . 11
3.3 Central B-splines . . . 13
3.4 Central spline filtering . . . 18
3.5 Central spline filtering of the DG approximation for a one-dimensional linear periodic problem . . . 24
3.6 Consequences for streamline visualisation . . . 25
3.7 Conclusion . . . 29

4 Conserving the convergence **31**
4.1 Introduction . . . 31
4.2 Auxiliary theory . . . 31
4.3 Error estimation for filtered functions in general . . . 34
4.4 Error estimation for filtered DG approximations . . . 39
4.5 Conclusion . . . 45

5 Conclusion **47**

Chapter 1

Introduction

The flexibility of the Discontinuous Galerkin (DG) method make it particularly suitable for obtaining higher-order approximatons of the solution to a hyperbolic system, such as the model of the flow around an air foil. This flexibility is a consequence of two main properties. First of all, unlike continuous Galerkin appoximations, DG approximations are allowed to be discontinuous along element boundaries. This makes the DG method particularly useful for modeling discontinuities such as shocks. Moreover, the DG convergence rate is not only determined by the element size and the accuracy of the numerical flux, but also by the degree of the polynomial space in which the solution is sought. Finite Volume methods and Finite Difference schemes do not share this virtue.

The computation of a DG approximation is often followed by a visualisation step, such as the computation of streamlines or isolines, to extract the features of the underlying physical phenomena that are of interest. Unfortunately, the aforementioned lack of smoothness of the DG method can hamper the accuracy of visualisation techniques. This literature study forms the start of a research that seeks to overcome this difficulty through smoothness-increasing convergence-conserving spline filtering. The main application is streamline visualisation, but other visualisation techniques may benefit as well from this research.

This report is organised as follows. First, a brief introduction to the hyperbolic systems under consideration, their Discontinuous Galerkin approximation and the visualisation of the results in the form of streamlines is provided (Chapter 2). After that, the one-dimensional central spline filter is defined and applied to a DG solution to enhance its smoothness (Chapter 3). For a certain class of linear periodic problems, it can be shown that the central spline filters at least preserve the order of convergence of the DG method (Chapter 4). Finally, a conclusion is given together with a list of future research questions (Chapter 5).

Chapter 2

Defining the problem

2.1 Introduction

This chapter briefly introduces the Discontinuous Galerkin (DG) method and the visualisation of its outcome in the form of streamlines for hyperbolic systems.

First, the weak formulation of non-linear hyperbolic systems is discussed (Section 2.2). The solution of these systems can be approximated by the DG method (Section 2.3). This method is considered in detail for a one-dimensional linear periodic example that will be revised in subsequent chapters. After that, the visualisation of DG approximations in the form of streamlines is discussed (Section 2.4), and a conclusion is given (Section 2.5).

2.2 Hyperbolic systems

Many physical phenomena, such as the flow around an air foil, are modeled in terms of hyperbolic systems, which are formulated in this section.

Any non-linear hyperbolic system (Definition 2.2) can also be formulated in a weak sense (Definition 2.3). The original so-called strong solution is also a weak solution, but the reverse implication is not valid in general (Proposition 2.5).

The next section formulates the DG method to approximate the weak solution.

Notation 2.1 ($\mathcal{L}^2$ inner product)
First, introduce the following notation for the standard $\mathcal{L}^2$ innner product:

$$\langle \underline{v}, \underline{w} \rangle_X = \int_X \underline{v}(\underline{x}) \cdot \underline{w}(\underline{x}) \, \mathrm{d}\underline{x}, \qquad \forall \underline{v}, \underline{w} \in \mathcal{L}^2(X, \mathbb{R}^D), \qquad \forall X \subseteq \mathbb{R}^d$$

For the sake of notational brevity, if X is a single element of $\mathbb{R}^d$, the integral is interpreted as the evaluation of the integrand in that element. ⌟

Definition 2.2 (Hyperbolic system - strong formulation)
Consider a time domain $T = [t_a, t_b]$, a compact connected spatial domain $X \subseteq \mathbb{R}^d$, a source function $\underline{g} \in \mathcal{C}^0(\mathbb{R}^D, \mathbb{R}^D)$, and flux functions $\underline{f}_q \in \mathcal{C}^1(\mathbb{R}^D, \mathbb{R}^d)$ (for all $q = 1, ..., D$). The *strong formulation* of a hyperbolic system describes a strong solution $\underline{u} \in \mathcal{C}^1(X \times T, \mathbb{R}^D)$ in terms of an initial condition, 'proper' boundary conditions, and an equation in the form

$$\frac{\partial \underline{u}(\underline{x}, t)}{\partial t} + \begin{bmatrix} \nabla_{\underline{x}} \cdot \Big(\underline{f}_1\big(\underline{u}(\underline{x}, t)\big) \Big) \\ \vdots \\ \nabla_{\underline{x}} \cdot \Big(\underline{f}_D\big(\underline{u}(\underline{x}, t)\big) \Big) \end{bmatrix} + \underline{g}\big(\underline{u}(\underline{x}, t)\big) = 0, \qquad \forall \underline{x} \in X, \qquad \forall t \in T. \tag{2.1}$$

See also [CJST98, p. 161, 201-202]. ⌟

Definition 2.3 (Hyperbolic system - weak formulation)
Consider Notation 2.1. The *weak formulation* of a hyperbolic system (Definition 2.2) describes a weak solution $\underline{u} \in \mathcal{C}^1\big(T, \mathcal{W}^{1,2}(X, \mathbb{R}^D)\big)$ that satisfies an initial condition, 'proper' boundary conditions, and:

$$\begin{aligned}\langle u_q(t), v(t)\rangle_X = \langle u_q(t_a), v(t_a)\rangle_X + \int_{t_a}^{t} \Bigg(&\left\langle u_q(\tau), \frac{\partial v}{\partial t}(\tau)\right\rangle_X \\ &+ \left\langle \underline{f}_q\big(\underline{u}(\tau)\big), \nabla_{\underline{x}} v(\tau)\right\rangle_X - \left\langle \underline{f}_q\big(\underline{u}(\tau)\big)\cdot \underline{n}, v(\tau)\right\rangle_{\partial X} \\ &- \left\langle g_q\big(\underline{u}(\tau)\big), v(\tau)\right\rangle_X \Bigg)\, \mathrm{d}\tau, \end{aligned} \tag{2.2}$$

for all test functions $v \in \mathcal{C}^1(T, \mathcal{C}^\infty(X))$, for all $t \in T$, and for all $q = 1, ..., D$. Here, $\underline{n}$ is the outward normal vector of the domain X. See also [CJST98, p. 161, 201-202]. ⌟

Example 2.4 (Periodic linear hyperbolic equation)
Consider a one-dimensional hyperbolic system (Definition 2.2 with $d, D = 1$) for a domain $X = [x_a, x_b]$. Suppose that the boundary conditions are periodic, the flux function is linear, and the source function is zero:

$$f(u) = cu, \qquad c > 0, \tag{2.3}$$
$$g(u) = 0. \tag{2.4}$$

Hence, the strong solution satisfies:

$$\frac{\partial u}{\partial t} + c\frac{\partial u}{\partial x} = 0.$$

The corresponding weak solution (Definition 2.3) satisfies periodic boundary conditions and

$$\begin{aligned}\langle u(t), v(t)\rangle_X = \langle u(t_a), v(t_a)\rangle_X + \int_{t_a}^{t} &\left\langle u(\tau), \frac{\partial v}{\partial t}(\tau) + c\frac{\partial v(\tau)}{\partial x}\right\rangle_X \mathrm{d}\tau \\ &+ \int_{t_a}^{t} \left(\left[cu(\tau)\, v(\tau)\right]_{x_a} + \left[-cu(\tau)\, v(\tau)\right]_{x_b}\right) \mathrm{d}\tau, \end{aligned} \tag{2.5}$$

for all test functions $v \in \mathcal{C}^1\big(T, \mathcal{C}^\infty(X)\big)$ and for all $t \in T$. ⌟

Proposition 2.5 (A strong solution is also a weak solution)
A strong solution (Definition 2.2) is also a weak solution (Definition 2.3).

PROOF:
See also [CJST98, p. 161, 201-202]. Consider the inner product of the strong formulation (2.1) with a smooth function $v \in \mathcal{C}^1(T, \mathcal{C}^\infty(X))$, integrate over the time interval $[t_a, t]$, and use integration by parts. This results in the weak formulation (2.2). ■

2.3 Discontinuous Galerkin method

The weak solution of a hyperbolic system, which was formulated in the previous section, can be approximated by means of the Discontinuous Galerkin (DG) method, which forms the subject of this section.

The DG method (Definition 2.7) can be seen as a combination of the finite volume method and the finite element method: it seeks a solution approximation that is a polynomial of a certain degree in each element of the mesh, and that is allowed to be discontinous along the element boundaries. An illustration of a possible outcome can be found in Figure 2.1. This figure illustrates the performance of the DG method for a one-dimensional periodic linear hyperbolic equation

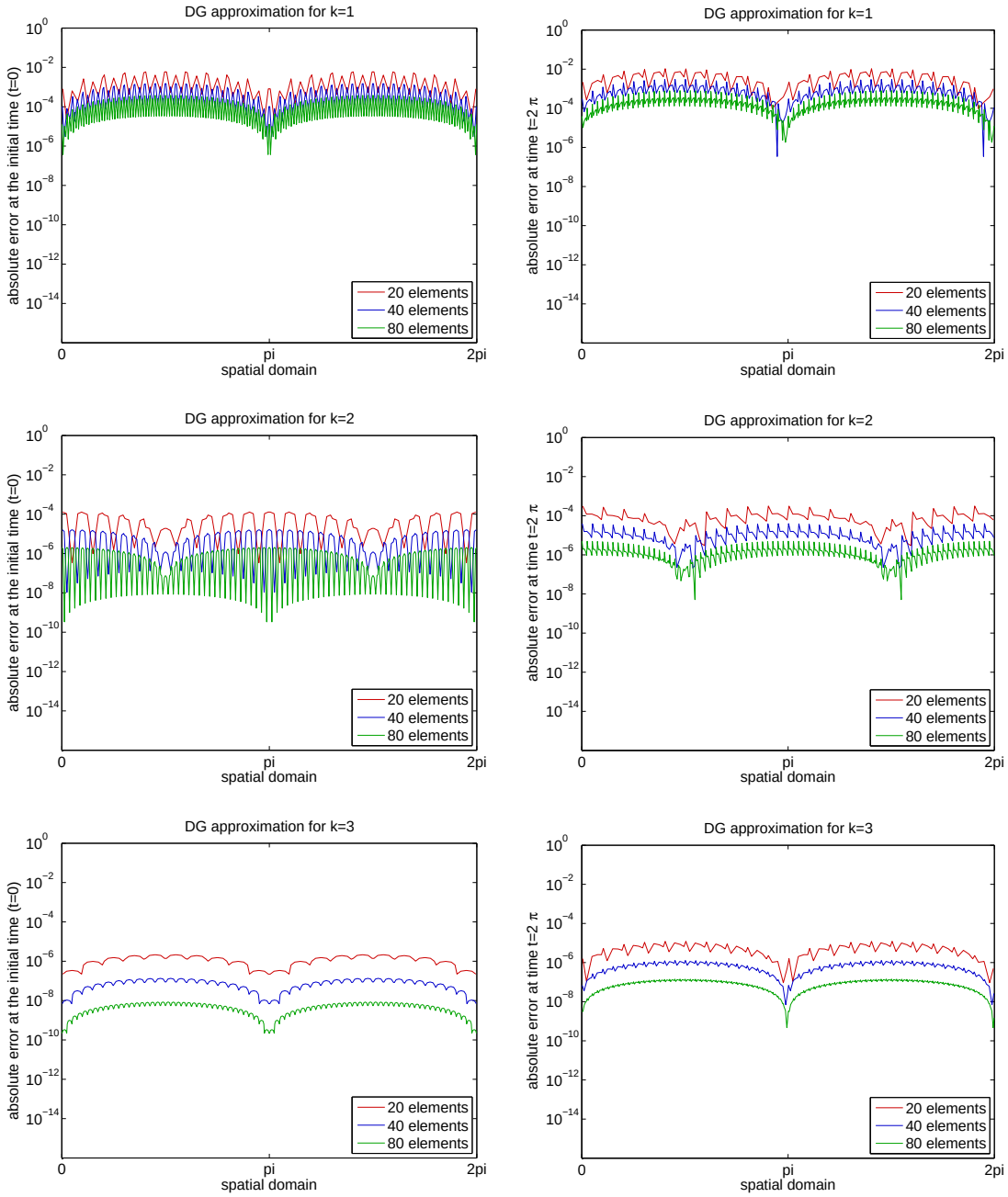

Figure 2.1: Absolute value of the error $|u - u_h|$ for a one-dimensional periodic linear hyperbolic problem (Example 2.9) with velocity $c = 1$ at the initial time (left) and after one period (right). The initial condition is the sine function and the time step equals $0.1h$. Notice that the convergence rate increases with the degree k of the polynomial space. Furthermore, observe the oscillatory nature of the error

using the first-order upwind flux function and the monomials as a polynomial basis (Example 2.8, (Example 2.9)).

Once the DG approximation has been obtained, a visualisation technique is usually required to extract the features of interest. This is the topic of the next section.

Notation 2.6 (Mesh, polynomial test space, etc.)
Consider Notation 2.1. First of all, let $\mathbb{N}_0 := \mathbb{N} \cup \{0\}$ denote the natural numbers including zero and $\mathbb{N}_1 := \mathbb{N} \backslash \{0\}$ the natural numbers excluding zero. For any compact connected domain $X \subseteq \mathbb{R}^d$ and corresponding mesh $\mathcal{X}_h = \{X_j \subseteq X\}_{j \in I \subseteq \mathbb{Z}}$ that consists of a finite number of closed sets with maximum diameter $h > 0$ that form a certain tesselation of X, introduce the following notation. For any linear subspace V of $\mathcal{L}^2(X)$, and for all $v \in \mathcal{L}^2(X)$, let $\mathbb{P}_V v$ denote the $\mathcal{L}^2$-projection of v onto V, i.e. $\langle \mathbb{P}_V v - v, w \rangle_X = 0$, for all $w \in V$. Furthermore, define the space of square-integrable functions that are piecewise polynomial:

$$\mathcal{P}^k_{\mathcal{X}_h}(X) := \left\{ v \in \mathcal{L}^2(X) \,:\, v|_{\mathrm{int}(X_j)} \in \mathcal{P}^k\big(\mathrm{int}(X_j)\big),\, \forall X_j \in \mathcal{X}_h \right\}, \qquad \forall k \in \mathbb{N}_0,$$

where $\mathrm{int}(X_j)$ denotes the interior of element X_j. The DG method makes use of test functions that are elements of a space of the latter kind. Additionally, introduce the space of square-integrable functions that are piecewise smooth:

$$\mathcal{C}^m_{\mathcal{X}_h}(X) := \left\{ v \in \mathcal{L}^2(X) \,:\, v|_{\mathrm{int}(X_j)} \in \mathcal{C}^m\big(\mathrm{int}(X_j)\big),\, \forall X_j \in \mathcal{X}_h \right\}, \qquad \forall m \in \mathbb{N}_0 \cup \{\infty\}.$$

Finally, for any piecwise continuous $v \in \mathcal{C}^0_{\mathcal{X}_h}(X)$, let v^j denote the unique continuous element of $\mathcal{C}^0(X_j)$ such that these two functions coincide in the interior of element X_j, i.e. $v^j|_{\mathrm{int}(X_j)} = v|_{\mathrm{int}(X_j)}$. ⌟

Definition 2.7 (Discontinuous Galerkin approximation)
Consider Notation 2.6. The Discontinuous Galerkin approximation of the weak solution (Definition 2.3) can be constructed in the following manner. Consider a mesh $\mathcal{X}_h = \{X_j \subseteq X\}_{j \in I \subseteq \mathbb{Z}}$ and let I_j contain the indices of the neighbors of element X_j:

$$I_j = \{m \in I \setminus \{j\} \,:\, e_{j,m} := \partial X_j \cap \partial X_m \neq \varnothing\}, \qquad \forall j \in I.$$

The *Discontinuous Galerkin approximation* $(u_h)_q \in \mathcal{C}^1\big(T, \mathcal{P}^k_{\mathcal{X}_h}(X)\big)$ to the exact solution u_q satisfies the boundary conditions of the weak formulation and:

$$\begin{aligned} \frac{d}{dt} \left\langle \left(u_h^j\right)_q (t), v^j \right\rangle_{X_j} &= \left\langle \underline{f}_q\big(\underline{u}_h^j(t)\big), \nabla_{\underline{x}} v^j \right\rangle_{X_j} - \sum_{m \in I_j} \left\langle \widetilde{f}_q\big(\underline{u}_h^j(t), \underline{u}_h^m(t)\big), v^j \right\rangle_{e_{j,m}} \\ &\quad - \left\langle g_q\big(\underline{u}_h^j(t)\big), v^j \right\rangle_{X_j}, \end{aligned} \tag{2.6}$$

for all test functions $v \in \mathcal{P}^k_{\mathcal{X}_h}(X)$, for all $t \in T$, for all $j \in I$, and for all $q = 1, ..., D$. Here, $\widetilde{f}_q : \mathbb{R}^D \times \mathbb{R}^D \to \mathbb{R}$ is a numerical flux function that is to be specified. The initial condition of the numerical approximation is the projection of the initial condition of the exact solution:

$$(u_h)_q(t_a) = \mathbb{P}_{\mathcal{P}^k_{\mathcal{X}_h}(X)}\big(u_q(t_a)\big), \qquad \forall q = 1, ..., D.$$

See also [CJST98, p. 161-163, 201-203]. ⌟

Example 2.8 (Periodic linear hyperbolic equation)
Consider Example 2.4. Choose points $x_a = x_{\frac{1}{2}} < x_{\frac{3}{2}} < ... < x_{J+\frac{1}{2}} = x_b$ in the domain and construct a mesh with these points:

$$\mathcal{X}_h = \{X_j := [x_{j-\frac{1}{2}}, x_{j+\frac{1}{2}}]\}_{j \in I := \{1,...,J\}},$$

with maximum diameter $h > 0$. Using the first-order upwind flux function,

$$\widetilde{f}(v, w) = cv,$$

the DG approximation (Definition 2.7) satisfies:

$$\frac{d}{dt}\left\langle u_h^j(t), v^j \right\rangle_{X_j} = \left\langle cu_h^j(t), \frac{\partial v^j}{\partial x} \right\rangle_{X_j} + \left[-cu_h^j(t)\, v^j\right]_{x_{j+\frac{1}{2}}} + \left[cu_h^{j'-1}(t)\, v^j\right]_{x_{j-\frac{1}{2}}}, \tag{2.7}$$

for all $v \in \mathcal{P}^k_{\mathcal{X}_h}(X)$, for all $t \in T$, and for all $j \in I$. Here,

$$j' := \begin{cases} j, & \text{for } j = 2, ..., J \\ J+1, & \text{for } j = 1, \end{cases}$$

in order to deal with the boundary conditions properly. ⌟

Example 2.9 (Computational aspects)
Consider Example 2.8. The solution to (2.7) can be computed with the help of a basis for the polynomial space $\mathcal{P}^k(X_j)$, such as the *monomials*:

$$v^{j,\ell}(x) = \left(\frac{x - \frac{x_{j-\frac{1}{2}} + x_{j+\frac{1}{2}}}{2}}{x_{j+\frac{1}{2}} - x_{j-\frac{1}{2}}} \right)^\ell, \qquad \forall x \in X_j, \qquad \forall \ell = 0, ..., k, \qquad \forall j \in I. \tag{2.8}$$

By writing the DG approximation as a linear combination of monomials,

$$u_h^j(t) = \sum_{\ell=0}^{k} C^{j,\ell}(t) v^{j,\ell}, \qquad \forall t \in T, \qquad \forall j \in I, \tag{2.9}$$

for certain unknown differentiable coefficients $C^{j,\ell}$, the DG method (2.7) can be formulated as follows:

$$\begin{aligned} \frac{d}{dt} \sum_{\ell=0}^{k} C^{j,\ell}(t) \left\langle v^{j,\ell}, v^{j,\ell'} \right\rangle_{X_j} = \sum_{\ell=0}^{k} \Bigg(& C^{j,\ell}(t) \left\langle v^{j,\ell}, \frac{\partial v^{j,\ell'}}{\partial x} \right\rangle_{X_j} \\ & - C^{j,\ell}(t) v^{j,\ell}(x_{j+\frac{1}{2}}) v^{j,\ell'}(x_{j+\frac{1}{2}}) \\ & + C^{j'-1,\ell}(t) v^{j'-1,\ell}(x_{j-\frac{1}{2}}) v^{j,\ell'}(x_{j-\frac{1}{2}}) \Bigg), \end{aligned}$$

for all $t \in T$, for all $\ell' = 0, ..., k$, and for all $j \in I$. This linear system of ODEs can also be written in matrix vector notation:

$$A^j \frac{d}{dt} \underline{c}^j(t) = B^{j,1} \underline{c}^j(t) + B^{j,2} \underline{c}^{j'-1}(t), \qquad \forall j \in I, \tag{2.10}$$

where $\underline{c}^j(t)$ is a vector of dimension $k+1$ that contains the coefficients used in the linear combination of polynomial basis functions (2.9):

$$c^j_{\ell+1}(t) = C^{j,\ell}(t), \qquad \forall j = 1, ..., J, \qquad \forall \ell = 0, ..., k,$$

and A^j, $B^{j,1}$ and $B^{j,2}$ are square matrices of dimension $(k+1)\times(k+1)$ with coefficients:

$$\begin{aligned}
A^j_{\ell'+1,\ell+1} &= \left\langle v^{j,\ell}, v^{j,\ell'} \right\rangle_{X_j} = \frac{\left(\frac{1}{2}\right)^{\ell+\ell'+1}\left(1+(-1)^{\ell+\ell'}\right)}{\ell+\ell'+1}(x_{j+\frac{1}{2}} - x_{j-\frac{1}{2}}),\\
B^{j,1}_{\ell'+1,\ell+1} &= \left\langle v^{j,\ell}, \frac{\partial v^{j,\ell'}}{\partial x} \right\rangle_{X_j} - v^{j,\ell}(x_{j+\frac{1}{2}})v^{j,\ell'}(x_{j+\frac{1}{2}})\\
&= \begin{cases} -\left(\frac{1}{2}\right)^{\ell}, & \ell'=0,\\ \frac{\ell'}{\ell+\ell'}\left(\left(\frac{1}{2}\right)^{\ell+\ell'} - \left(\frac{1}{2}\right)^{\ell+\ell'}\right) - \left(\frac{1}{2}\right)^{\ell+\ell'}, & \text{else,}\end{cases}\\
B^{j,2}_{\ell'+1,\ell+1} &= v^{j'-1,\ell}(x_{j-\frac{1}{2}})v^{j,\ell'}(x_{j-\frac{1}{2}}) = \left(\frac{1}{2}\right)^{\ell}\left(-\frac{1}{2}\right)^{\ell'},
\end{aligned}$$

for all $\ell,\ell' = 0,...,k$ and for all $j\in I$. Because the initial condition of $u^j_h(t_a)$ is the projection of the initial condition of the exact solution $u^j(t_a)$ onto the polynomial space $\mathcal{P}^k(X_j)$ in the $\mathcal{L}^2$-norm, the initial condition for the coefficients follows from:

$$A^j \underline{c}^j(t_a) = \underline{b}^j,$$

where $\underline{b}^j$ is a vector of dimension $k+1$ with coefficients

$$b^j_{\ell'+1} = \int_{x_{j-\frac{1}{2}}}^{x_{j+\frac{1}{2}}} u(x,t_a)v^{j,\ell'}(x)\,\mathrm{d}x, \qquad \forall j\in I, \qquad \forall \ell' = 0,...,k.$$

Finally, this linear system of ODEs can be solved by a numerical ODE solver, such as the third-order TVD-Runge-Kutta method (Definition 2.12). This literature study leaves the motivation for the particular choice for an ODE solver out of consideration. By substituting the resulting coefficients into the linear combination of monomials (2.9), the final DG approximation is obtained. For an illustration of the error of such an approximation, see Figure 2.1. ⌟

2.4 Visualisation of the results as streamlines

The previous section discussed the DG method for hyperbolic problems. Such a computation can be followed by a visualisation step to extract the features of the underlying physical phenomena that are of interest. An example of such a technique is the visualisation of a vector field, such as the flow around an airfoil, in the form of streamlines, which forms the subject of this section.

A streamline of a vector field is a line that is tangent to that field everywhere (Definition 2.10). A streamline through a certain location can be computed by means of a one-dimensional ODE-solver that uses that location as an initial condition. Examples of such solvers are the Euler Forward scheme (Definition 2.11) and the third-order TVD-Runge-Kutta scheme (Definition 2.12). An illustration of six vector field visualisation techniques, including two streamline visualisation techniques, can be found in Figure 2.2.

The results of Laidlaw et al. [LKJ+05] suggest that streamline visualisation techniques are preferred over other vector field visualisation techniques for critical point type identification and particle path prediction. Another advantage of streamlines is that they are applicable for both two- and three-dimensional fields.

Unfortunately, many ODE solvers assume that the field that they are acting upon is smooth, as such solvers are often based on Taylor series. At the same time, DG approximations are usually discontinuous along element boundaries. This lack of smoothness does not benefit the accuracy of the streamline visualisation. Which level of differentiability is required *exactly* is unclear at this point, and most likely depends on the ODE solver under consideration.

The next chapter seeks to enhance the smoothness of a DG approximation through central spline filtering.

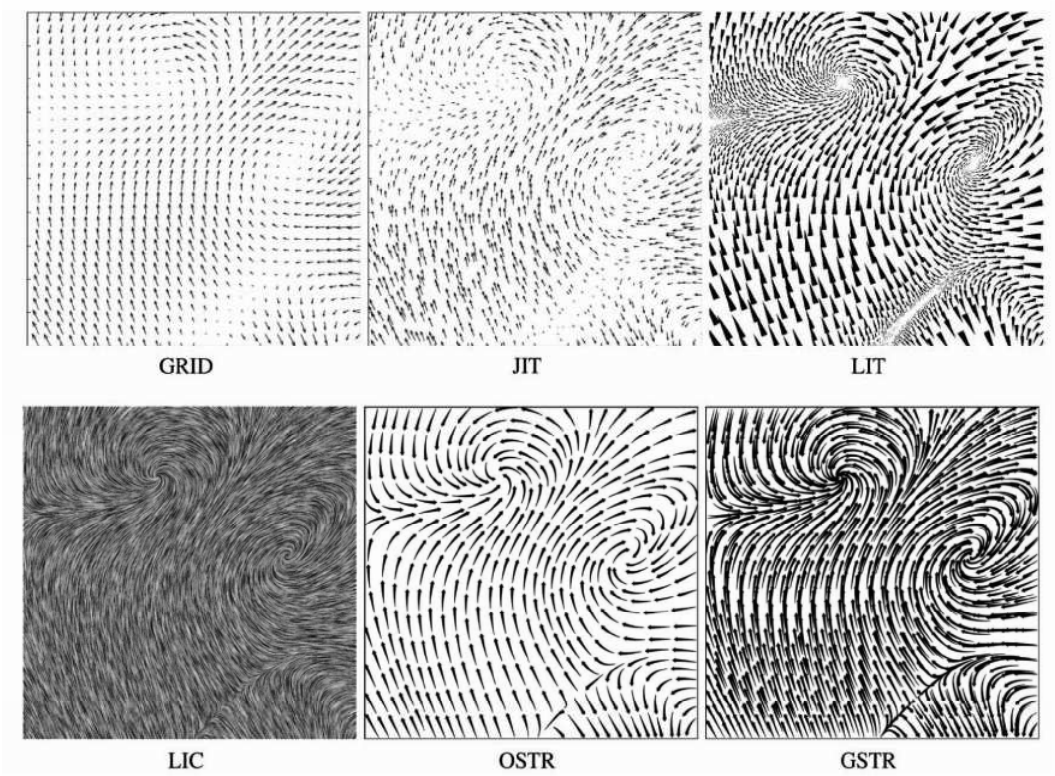

Figure 2.2: Visualisation of a vector field using six different techniques as published in [LKJ+05]: unlike the other four techniques, OSTR and GSTR are streamline visualisation methods. The results of Laidlaw et al. [LKJ+05] suggest that these two streamline visualisation techniques are preferred for critical point type identification and particle path prediction.

Definition 2.10 (Streamline)
Consider a domain $X \subseteq \mathbb{R}^d$. A *streamline* of an integrable vector field $\underline{u} : X \to \mathbb{R}^D$ through $\underline{x}_0 \in X$ is a curve $\underline{y} \in \mathcal{C}^1([\lambda_a, \lambda_b], \mathbb{R}^d)$ that is tangent to the vector field, i.e. which satisfies:

$$\underline{y}(\lambda) = \underline{y}(\lambda_a) + \int_{\lambda_a}^{\lambda} \underline{u}(\underline{y}(\lambda))\,\mathrm{d}\lambda, \qquad \forall \lambda \in [\lambda_a, \lambda_b], \qquad \underline{y}(\lambda_a) = \underline{x}_0. \tag{2.11}$$

See also [WRKH09, Section 3]. ⌟

Definition 2.11 (Euler forward)
The *Euler forward* scheme describes a numerical solution to (2.11) in the following manner:

$$\begin{aligned} \underline{y}^0 &= \underline{y}(\lambda_a) = \underline{x}_0, \\ \underline{y}(\lambda_j) \approx \underline{y}^j &= \underline{y}^{j-1} + (\lambda_j - \lambda_{j-1})\,\underline{u}(\underline{y}^{j-1}), \end{aligned}$$

for all $j = 1, ..., J$, and with $\lambda_a = \lambda_0 < \lambda_1 < ... < \lambda_J = \lambda_b$. ⌟

Definition 2.12 (Third-order TVD-Runge-Kutta)
The *third-oder TVD-Runge-Kutta* scheme describes a numerical solution to (2.11) in the following

manner:

$$\begin{aligned}
\underline{y}^0 &= \underline{y}(\lambda_a) = \underline{x}_0, \\
\underline{y}^{j,0} &= \underline{y}^{j-1}, \\
\underline{y}^{j,1} &= \underline{y}^{j,0} + (\lambda_j - \lambda_{j-1})\,\underline{u}(\underline{y}^{j,0}), \\
\underline{y}^{j,2} &= \frac{3}{4}\underline{y}^{j,0} + \frac{1}{4}\underline{y}^{j,1} + \frac{1}{4}(\lambda_j - \lambda_{j-1})\,\underline{u}(\underline{y}^{j,1}), \\
\underline{y}^{j,3} &= \frac{1}{3}\underline{y}^{j,0} + \frac{2}{3}\underline{y}^{j,2} + \frac{2}{3}(\lambda_j - \lambda_{j-1})\,\underline{u}(\underline{y}^{j,2}), \\
\underline{y}(\lambda_j) \approx \underline{y}^j &= \underline{y}^{j,3},
\end{aligned}$$

for all $j = 1, ..., J$, and with $\lambda_a = \lambda_0 < \lambda_1 < ... < \lambda_J = \lambda_b$. See also [CJST98, p. 170,171]. ⌟

2.5 Conclusion

The Discontinuous Galerkin (DG) method is a flexible method for approximating the solution of a hyperbolic system. Its flexibility is mostly due to the fact that its outcome is allowed to be discontinuous at the element boundaries. This can in turn become a disadvantage, since a lack of smoothness can have a negative effect on streamline visualisation techniques. The main goal of this research is to tackle this problem through spline filtering, which is discussed in the next chapter.

Chapter 3

Increasing the smoothness

3.1 Introduction

The previous chapter mentioned why a lack of smoothness of a DG approximation can hamper its visualisation in the form of streamlines. This problem can be tackled through spline filtering, which is the subject of this chapter.

First, the definition and properties of B-splines are given, as these form the building blocks of spline filters (Section 3.2). This report focusses on so-called central spline filters (Section 3.4), which convolve the function to be filtered against a certain linear combination of central B-splines (Section 3.3). The smoothing effect of this filter on DG solutions is illustrated for a one-dimensional linear periodic problem (Section 3.5). After discussing the consequences for streamline visualisation (Section 3.6), a conclusion is given (Section 3.7).

3.2 B-splines

B-splines form the core elements of spline filters. For this reason, their definition and properties are considered in this section.

Because the divided difference of a polynomial of sufficiently low degree is equal to zero (Proposition 3.2), Peano's theorem can be applied for divided differences (Theorem 3.3). This basically implies that the divided difference of a function can be expressed in terms of the integral over the product of a derivative of that function and what will be defined as a B-spline (Definition 3.4). It can be shown that a B-spline is a spline with compact support (Proposition 3.6). A spline is a piecewise polynomial of a certain smoothness (Definition 3.5).

This report considers spline filters that are based on so-called central B-splines, which are discussed in the next section.

Notation 3.1 (Divided differences etc.)
First, define the following functions

$$\begin{aligned} \eta(x,\xi) &:= \xi - x, && \forall x,\xi \in \mathbb{R} \\ x_+^s &:= (\max\{x,0\})^s, && \forall x \in \mathbb{R}, \qquad \forall s \in \mathbb{N}_0, \qquad 0^0 := 0. \end{aligned} \tag{3.1}$$

Furthermore, for all functions $v : \mathbb{R} \to \mathbb{R}$, let

$$v([x_0,...,x_s]) = \sum_{j=0}^{s} \frac{v(x_j)}{\prod_{m\in\{0,...,s\}\setminus\{j\}}(x_j - x_m)}, \qquad \forall s \in \mathbb{N}_1,$$

denote the *divided difference* with respect to points $x_0,...,x_s \in \mathbb{R}$, and let

$$\partial_H v(x) = \frac{v(x+\frac{H}{2}) - v(x-\frac{H}{2})}{H}, \qquad \forall x \in \mathbb{R},$$

denote the *central difference quotient* with respect to a scale $H > 0$. ⌟

Proposition 3.2 (Divided difference of a polynomial)
Consider Notation 3.1, let $s \in \mathbb{N}_1$, and let $m \in \mathbb{N}_0$. The divided difference with respect to points $x_0, ..., x_s \in \mathbb{R}$ of a polynomial of degree $s-1$ or lower is equal to zero:

$$p([x_0, ..., x_s]) = 0, \qquad \forall p \in \mathcal{P}^{s-1}(\mathbb{R}).$$

PROOF:
The mean value theorem for divided differences implies that there exists $\xi \in \mathbb{R}$ such that:

$$p([x_0, ..., x_s]) = \frac{1}{s!} \frac{d^s p}{dx^s}(\xi). \tag{3.2}$$

The latter term is zero, because the s^{th} order derivative of a polynomial of degree $s-1$ or lower is equal to zero. ■

Theorem 3.3 (Peano's theorem (special case))
Consider Notation 3.1, let $s \in \mathbb{N}_1$ and suppose that $x_0 < ... < x_s \in \mathbb{R}$. Furthermore, define:

$$\psi^s(x) := s\eta_+^{s-1}(x, [x_0, ..., x_s]) = s \sum_{j=0}^{s} \frac{(x_j - x)_+^{s-1}}{\prod_{m \in \{0,...,s\} \setminus \{j\}} (x_j - x_m)}, \qquad \forall x \in \mathbb{R}. \tag{3.3}$$

Then,

$$\int_{x_0}^{x_s} \frac{d^s v(x)}{dx^s} \psi^s(x) \, \mathrm{d}x = s! v([x_0, ..., x_s]), \qquad \forall v \in \mathcal{C}^s[x_0, x_s].$$

PROOF:
Because of Proposition 3.2, the claim follows from Peano's theorem. For the proof of the latter, see e.g. [Dav75, Theorem 3.7.1]. ■

Definition 3.4 (B-spline)
A *B-spline* of degree $s \in \mathbb{N}_1$ with knots $x_0 < ... < x_s$ is a function $\psi^s : \mathbb{R} \to \mathbb{R}$ of the form (3.3). See also [Sch73, p. 2]. ⌟

Definition 3.5 (Spline)
A (polynomial) *spline* of degree $s \in \mathbb{N}_1$ with knots $x_0 < ... < x_s$ is a function $\phi : \mathbb{R} \to \mathbb{R}$ that is a piecewise polynomial in the sense that, for each open interval between the knots, i.e. for each

$$X \in \big\{(-\infty, x_1), (x_0, x_1), ..., (x_{s-1}, x_s), (x_s, \infty)\big\},$$

there exists a polynomial $p \in \mathcal{P}^{s-1}(X)$ such that

$$\phi(x) = p(x), \qquad \forall x \in X,$$

and that is smooth in the sense that $\phi \in \mathcal{C}^{s-2}(\mathbb{R})$, as long as $s \geq 2$. If $s = 1$, discontinuities at the knots are allowed. See also [Sch73, p. 1], [Sch81, p.108], and [Nür89, p. 94, 96]. ⌟

Proposition 3.6 (B-splines are splines with compact support)
A B-spline $\psi^s(x)$ of degree $s \in \mathbb{N}_1$ with knots $x_0 < ... < x_s$ (Definition 3.4) is a spline of degree s with knots $x_0 < ... < x_s$ (Definition 3.5) that is zero outside of $[x_0, x_s]$. Moreover,

$$\int_{\mathbb{R}} \psi^s(x) \, \mathrm{d}x = 1. \tag{3.4}$$

PROOF:
See also [Sch73, p. 2,3] and [CS66, p. 73-75]. Consider Notation 3.1. With the help of Proposition 3.2, substitution of

$$\eta_+^{s-1} = \eta^{s-1} + (-1)^s(-\eta)_+^{s-1},$$

into (3.3) leads to the following alternative formulation of the B-spline:

$$\psi^s(x) = s(-1)^s \sum_{j=0}^{s} \frac{(x - x_j)_+^{s-1}}{\prod_{m\in\{0,\dots,s\}\setminus\{j\}}(x_j - x_m)}. \tag{3.5}$$

Now, (3.3) and (3.5) imply that the B-spline is zero for $x > x_s$ and $x < x_0$ respectively. Rewriting (3.3) gives that the B-spline is a polynomial of degree $s-1$ inside each open interval between the knots:

$$\psi^s(x) = s \sum_{j=q}^{s} \frac{(x_j - x)^{s-1}}{\prod_{m\in\{0,\dots,s\}\setminus\{j\}}(x_j - x_m)}, \qquad \forall x \in (x_q, x_{q+1}), \qquad \forall q = 0, \dots, s-1.$$

Furthermore, note that the B-spline is continuous if $s \geq 2$. Finally, it is shown that $\psi^s \in \mathcal{C}^{s-2}(\mathbb{R})$, for $s \geq 3$. To this end compute the derivatives inside the open intervals:

$$\frac{d^\ell \psi^s(x)}{dx^\ell} = (-1)^\ell (\ell-1)! \sum_{j=q}^{s} \frac{(x_j - x)^{s-1-\ell}}{\prod_{m\in\{0,\dots,s\}\setminus\{j\}}(x_j - x_m)},$$

for all $x \in (x_q, x_{q+1})$, for all $q = 0, \dots, s-1$, for all $\ell = 1, \dots, s-2$. Observing the limits in the knots,

$$\lim_{x\uparrow x_j} \frac{d^\ell \psi^s(x)}{dx^\ell} = \lim_{x\downarrow x_j} \frac{d^\ell \psi^s(x)}{dx^\ell}, \qquad \forall j = 0, \dots, s,$$

shows that $\psi^s \in \mathcal{C}^{s-2}(\mathbb{R})$, for $s \geq 3$. Finally, the fact that

$$\int_{\mathbb{R}} \psi^s(x)\,\mathrm{d}x = 1.$$

follows from Theorem 3.3 for $v(x) = x^s$ and (3.2). ∎

3.3 Central B-splines

The previous section formulated B-splines and discussed some of their properties, which form the buiding blocks of spline filters. This report considers central spline filters that are based on so-called central B-splines, which are discussed in this section.

Central B-splines are B-splines whose knots are sampled in a symmetric and equidistant fashion (Definition 3.7, Figure 3.1). They can be formulated in three equivalent ways (Proposition 3.8 and Proposition 3.9), which each help to reveal different properties. One of these is that their derivatives can be expressed in terms of central difference quotients of lower order central B-splines (Proposition 3.11, Proposition 3.12). This property plays an important role in the convergence analysis in the next chapter.

The next section defines central spline filters in terms of a linear combination of central B-splines.

Definition 3.7 (Central B-spline)
A *central B-spline* of degree $s \in \mathbb{N}_1$ is a B-spline (Definition 3.4) with knots $\{x_j = -\frac{s}{2} + j\}_{j=0,\dots,s}$. In the remainder of this report, the following notation will be tacitly assumed:

$$\psi_H^s(x) := \frac{1}{H}\psi^s\left(\frac{x}{H}\right), \qquad \forall x \in \mathbb{R}, \qquad \forall H > 0.$$

See also [Sch73, p. 11]. ⌟

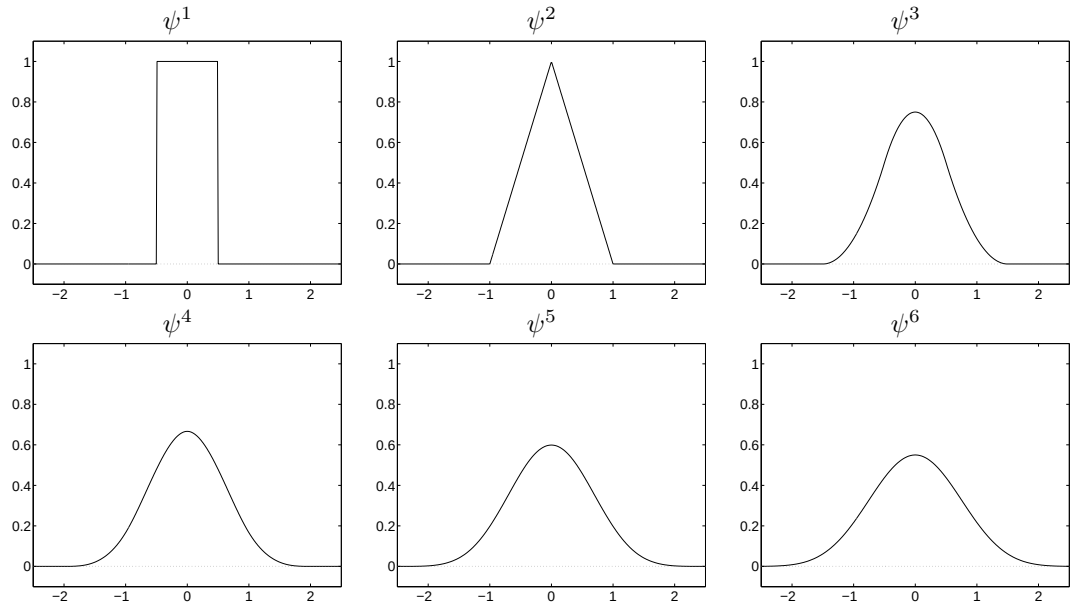

Figure 3.1: Central B-splines (Definition 3.7): the core elements of the central spline filters are formed by the central B-splines. Notice that, as the order increases, the smoothness and the support increase and the maximum value of the B-spline decreases.

Proposition 3.8 (Divided difference of a product)
Consider Notation 3.1, let $J \in \mathbb{N}_1$ and suppose that $x_0, ..., x_J \in \mathbb{R}$. Furthermore, consider $v, w : \mathbb{R} \to \mathbb{R}$. Then, the divided difference of the product of these functions can be expressed as the following sum:

$$(vw)[x_0, ..., x_J] = \sum_{j=0}^{J} v[x_0, ..., x_j] w[x_j, ..., x_J].$$

PROOF:
See e.g. [Sch81, Theorem 5.52]. ∎

Proposition 3.9 (Three equivalent formulations of central B-splines)
Consider Notation 3.1. Central B-splines (Definition 3.7) of degree $s \in \mathbb{N}_1$ can be formulated in terms of

1. divided differences:

$$\psi^s(x) = s\eta_+^{s-1}\left(x, \left[-\frac{s}{2}, ..., \frac{s}{2}\right]\right) \tag{3.6}$$

$$= s\sum_{j=0}^{s} \frac{\left(-\frac{s}{2} + j - x\right)_+^{s-1}}{\prod_{m\in\{0,...,s\}\setminus\{j\}}(j-m)} \tag{3.7}$$

$$= s\sum_{j=0}^{s} (-1)^{j-s} \frac{\left(-\frac{s}{2} + j - x\right)_+^{s-1}}{j!(s-j)!}; \tag{3.8}$$

2. recursive convolutions of an indicator function with itself:

$$\psi^1(x) = \mathbb{1}_{[-\frac{1}{2},\frac{1}{2})}(x),$$
$$\psi^s(x) = (\psi^1 \star \psi^{s-1})(x) := \int_{-\infty}^{\infty} \psi^1(\xi)\psi^{s-1}(x-\xi)\,\mathrm{d}\xi, \qquad s = 2, 3, ...; \tag{3.9}$$

3. recursion relations:

$$\psi^1(x) = \mathbb{1}_{[-\frac{1}{2},\frac{1}{2})}(x),$$
$$\psi^s(x) = \frac{(\frac{s}{2}+x)\psi^{s-1}(x+\frac{1}{2}) + (\frac{s}{2}-x)\psi^{s-1}(x-\frac{1}{2})}{s-1}, \qquad s = 2, 3, \ldots . \tag{3.10}$$

From the latter form it becomes clear that central B-splines are even functions.

PROOF:
See also [Sch73, p. 11,12] and [Sch81, Theorem 4.15]. Formulation (3.7) is a special case of (3.3). To show that this formulation is equivalent to (3.9), first observe that the equivalence applies for $s = 1$. For $s \geq 2$, apply Peano's theorem (Theorem 3.3) to obtain:

$$\int_{-\frac{s}{2}}^{\frac{s}{2}} \frac{d^s v(x)}{dx^s} \psi^s(x)\,\mathrm{d}x = \partial_1^s v(0), \qquad \forall v \in \mathcal{C}^s(\mathbb{R}).$$

For $v(x) = e^{ix\xi}$, this leads to

$$(i\xi)^s \int_{-\frac{s}{2}}^{\frac{s}{2}} e^{ix\xi}\psi^s(x)\,\mathrm{d}x = \left(2i\sin\left(\frac{1}{2}\xi\right)\right)^s.$$

Because the central B-spline is zero outside of the interval $[-\frac{s}{2}, \frac{s}{2}]$ (cf. Proposition 3.6), the Fourier transform is obtained:

$$\mathscr{F}\{\psi^s\}(\xi) = \int_{-\infty}^{\infty} e^{ix\xi}\psi^s(x)\,\mathrm{d}x = \left(\frac{\sin\left(\frac{1}{2}\xi\right)}{\frac{1}{2}\xi}\right)^s,$$

This can be worked out further to get:

$$\begin{aligned}
\mathscr{F}\{\psi^s\}(\xi) &= \left(\frac{\sin\left(\frac{1}{2}\xi\right)}{\frac{1}{2}\xi}\right)^s \\
&= \left(\frac{\sin\left(\frac{1}{2}\xi\right)}{\frac{1}{2}\xi}\right)^{s-1}\left(\frac{\sin\left(\frac{1}{2}\xi\right)}{\frac{1}{2}\xi}\right)^1 \\
&= \mathscr{F}\{\psi^{s-1}\}(\xi)\mathscr{F}\{\psi^1\}(\xi) \\
&= \mathscr{F}\{\psi^{s-1} \star \psi^1\}(\xi)
\end{aligned}$$

Applying the inverse Fourier transform gives (3.9). The equivalence of (3.7) and (3.10) can be shown as follows. First, observe that the equivalence applies for $s = 1$. For $s \geq 2$, rewrite (3.3) by observing that $x_+^{s-1} = x x_+^{s-2}$:

$$\psi^s(x) = s(\eta\eta_+^{s-2})(x, [x_0, ..., x_s]).$$

Next, apply Proposition 3.8:

$$\psi^s(x) = s\sum_{j=0}^{s} \eta(x, [x_0, ..., x_j])\eta_+^{s-2}(x, [x_j, ..., x_s]).$$

Because of Proposition 3.2, this sum can be truncated:

$$\begin{aligned}
\psi^s(x) =& s\Big(\eta(x, [x_0])\eta_+^{s-2}(x, [x_0, ..., x_s]) + \eta(x, [x_0, x_1])\eta_+^{s-2}(x, [x_1, ..., x_s])\Big) \\
=& s\Bigg(\eta(x, x_0)\frac{\eta_+^{s-2}(x, [x_1, ..., x_s]) - \eta_+^{s-2}(x, [x_0, ..., x_{s-1}])}{x_s - x_0} \\
&+ \frac{\eta(x, x_1) - \eta(x, x_0)}{x_1 - x_0}\eta_+^{s-2}(x, [x_1, ..., x_s])\Bigg).
\end{aligned}$$

Next, use the fact that $x_j = -\frac{s}{2} + j$ to obtain the following expressions for the lower order central B-spline:

$$\begin{aligned}
\psi^s(x) &= (s-1)\eta_+^{s-2}\left(x, \left[x_0 + \frac{1}{2}, ..., x_s - \frac{1}{2}\right]\right), \\
\psi^s\left(x + \frac{1}{2}\right) &= (s-1)\eta_+^{s-2}\left(x, [x_0, ..., x_{s-1}]\right), \\
\psi^s\left(x - \frac{1}{2}\right) &= (s-1)\eta_+^{s-2}\left(x, [x_1, ..., x_s]\right).
\end{aligned}$$

Substitution of these expressions, the values of the knots $x_j = -\frac{s}{2} + j$, and $\eta(x, \xi) = \xi - x$ yields:

$$\begin{aligned}
\psi^s(x) &= \frac{s}{s-1}\left((-\frac{s}{2} - x)\frac{\psi^s\left(x - \frac{1}{2}\right) - \psi^s\left(x + \frac{1}{2}\right)}{s} + \frac{(-\frac{s}{2} + 1 - x) - (-\frac{s}{2} - x)}{1}\psi^s\left(x - \frac{1}{2}\right)\right) \\
&= \frac{(\frac{s}{2} + x)\psi^s\left(x + \frac{1}{2}\right) + (\frac{s}{2} - x).\psi^s\left(x - \frac{1}{2}\right)}{s-1},
\end{aligned}$$

which completes the proof. ∎

Example 3.10 (Three central B-splines)
Examples of central B-splines are:

$$\psi^1(x) = \begin{cases} 1, & x \in \left[-\frac{1}{2}, \frac{1}{2}\right), \\ 0, & \text{else}, \end{cases}$$

$$\psi^2(x) = \begin{cases} x + 1, & x \in [-1, 0), \\ -x + 1, & x \in [0, 1), \\ 0, & \text{else}, \end{cases}$$

$$\psi^3(x) = \begin{cases} \frac{1}{2}x^2 + \frac{3}{2}x + \frac{9}{8}, & x \in \left[-\frac{3}{2}, -\frac{1}{2}\right), \\ -x^2 + \frac{3}{4}, & x \in \left[\frac{1}{2}, \frac{1}{2}\right), \\ \frac{1}{2}x^2 - \frac{3}{2}x + \frac{9}{8}, & x \in \left[\frac{1}{2}, \frac{3}{2}\right), \\ 0, & \text{else}. \end{cases}$$

For an illustration, see Figure 3.1. ⌟

Proposition 3.11 (Derivatives of a central B-spline)
Let ψ^s denote the central B-spline (Definition 3.7) of degree $s \geq 3$. Then, for $\alpha \in \{1, ..., s-2\}$, the α^{th} order derivative of the (scaled) central B-spline can be expressed in terms of central difference quotients of lower order B-splines:

$$\frac{d^\alpha \psi_H^s}{dx^\alpha}(x) = \partial_H^\alpha \psi_H^{s-\alpha}(x), \qquad \forall x \in \mathbb{R}, \qquad \forall H > 0. \tag{3.11}$$

Proof:
See also [Sch73, p. 12]. First of all, note that the α^{th} order derivative of the central B-spline ψ^s exists, since $\psi^s \in \mathcal{C}^{s-2}(\mathbb{R})$ (cf. Proposition 3.6). For the non-scaled central B-spline, the first-order

derivative can be computed as follows:

$$\begin{aligned}
\frac{d\psi^s}{dx}(x) &\overset{(3.9)}{=} \frac{d\left(\psi^{s-1} \star \psi^1\right)}{dx}(x) \\
&= \frac{d}{dx}\left(\int_{-\frac{1}{2}}^{\frac{1}{2}} \psi^{s-1}(x-\xi)\,\mathrm{d}\xi\right) \\
&= \frac{d}{dx}\left(\int_{x-\frac{1}{2}}^{x+\frac{1}{2}} \psi^{s-1}(\xi)\,\mathrm{d}\xi\right) \\
&= \psi^{s-1}\left(x+\frac{1}{2}\right) - \psi^{s-1}\left(x-\frac{1}{2}\right) \\
&= \partial_1 \psi^{s-1}(x), \qquad\qquad \forall x \in \mathbb{R}.
\end{aligned}$$

For the scaled central B-spline, this leads to:

$$\begin{aligned}
\frac{d\psi_H^s}{dx}(x) &= \frac{1}{H^2}\frac{d\psi^s}{dx}\left(\frac{x}{H}\right) \\
&= \frac{1}{H^2}\left(\psi^{s-1}\left(\frac{x}{H}+\frac{1}{2}\right) - \psi^{s-1}\left(\frac{x}{H}-\frac{1}{2}\right)\right) \\
&= \frac{1}{H}\left(\psi_H^{s-1}\left(x+\frac{H}{2}\right) - \psi_H^{s-1}\left(x-\frac{H}{2}\right)\right) \\
&= \partial_H \psi_H^{s-1}(x), \qquad\qquad \forall x \in \mathbb{R}.
\end{aligned}$$

Repetitive application of this result completes the proof. ∎

Proposition 3.12 (Derivatives of convolutions against a central B-spline)
Let ψ^s denote the central B-spline (Definition 3.7) of degree $s \geq 1$, and let ψ^0 denote the dirac distribution. Furthermore, let $u \in \mathcal{C}_0^\infty(\mathbb{R})$ and let $\alpha \in \{0, ..., s\}$. Then,

$$\frac{d^\alpha\left(\psi_H^s \star u\right)}{dx^\alpha}(x) = \left(\psi_H^{s-\alpha} \star \partial_H^\alpha u\right)(x), \qquad \forall x \in \mathbb{R}, \qquad \forall H > 0. \tag{3.12}$$

Proof:
The case $\alpha = 0$ is trivial. Next, for the case $\alpha = 1$, the claim is shown for $s = 1$, $s = 2$, and $s \geq 3$ subsequently. For $s = 1$,

$$\begin{aligned}
\frac{d\left(\psi_H^1 \star u\right)}{dx}(x) &= \left(\psi_H^1 \star \frac{du}{dx}\right)(x) \\
&= \int_{\mathbb{R}} \psi_H^1(\xi)\frac{du}{dx}(x-\xi)\,\mathrm{d}\xi \\
&= \frac{1}{H}\int_{\mathbb{R}} \psi^1\left(\frac{\xi}{H}\right)\frac{du}{dx}(x-\xi)\,\mathrm{d}\xi \\
&= \int_{\mathbb{R}} \psi^1(\xi)\,\frac{du}{dx}(x-H\xi)\,\mathrm{d}\xi \\
&= \int_{-\frac{1}{2}}^{\frac{1}{2}} \frac{du}{dx}(x-H\xi)\,\mathrm{d}\xi \\
&= \left[-\frac{1}{H}u(x-H\xi)\right]_{-\frac{1}{2}}^{\frac{1}{2}} \\
&= \partial_H u(x) \\
&= \left(\psi_H^0 \star \partial_H u\right)(x), \qquad\qquad \forall x \in \mathbb{R}, \qquad \forall H > 0.
\end{aligned}$$

For $s = 2$,

$$\begin{aligned}\frac{d\left(\psi_H^2 \star u\right)}{dx}(x) &= \left(\psi_H^2 \star \frac{du}{dx}\right)(x) \\ &= \int_{\mathbb{R}} \psi_H^2(\xi) \frac{du}{dx}(x-\xi)\,\mathrm{d}\xi \\ &= \frac{1}{H}\int_{\mathbb{R}} \psi^2\left(\frac{\xi}{H}\right)\frac{du}{dx}(x-\xi)\,\mathrm{d}\xi \\ &= \int_{\mathbb{R}} \psi^2(\xi)\,\frac{du}{dx}(x-H\xi)\,\mathrm{d}\xi \\ &= \int_{-1}^{0}(\xi+1)\frac{du}{dx}(x-H\xi)\,\mathrm{d}\xi + \int_{0}^{1}(-\xi+1)\frac{du}{dx}(x-H\xi)\,\mathrm{d}\xi, \quad \forall x\in\mathbb{R}, \quad \forall H>0.\end{aligned}$$

Applying partial integration yields:

$$\begin{aligned}\frac{d\left(\psi_H^2 \star u\right)}{dx}(x) = &\left[-\frac{1}{H}(\xi+1)u(x-H\xi)\right]_{-1}^{0} + \frac{1}{H}\int_{-1}^{0} u(x-H\xi)\,\mathrm{d}\xi \\ &\left[-\frac{1}{H}(-\xi+1)u(x-H\xi)\right]_{0}^{1} - \frac{1}{H}\int_{0}^{1} u(x-H\xi)\,\mathrm{d}\xi, \quad \forall x\in\mathbb{R}, \quad \forall H>0.\end{aligned}$$

The first and third term cancel. A change of variables yields for the other two terms:

$$\begin{aligned}\frac{d\left(\psi_H^2 \star u\right)}{dx}(x) =& -\frac{1}{H^2}\int_{x-\frac{H}{2}}^{x+\frac{H}{2}} u\left(\xi-\frac{H}{2}\right)\mathrm{d}\xi + \frac{1}{H^2}\int_{x-\frac{H}{2}}^{x+\frac{H}{2}} u\left(\xi+\frac{H}{2}\right)\mathrm{d}\xi \\ =&\frac{1}{H}\int_{x-\frac{H}{2}}^{x+\frac{H}{2}} \partial_H u(\xi)\,\mathrm{d}\xi \\ =&\left(\psi_H^1 \star \partial_H u\right)(x), \qquad \forall x\in\mathbb{R}, \quad \forall H>0.\end{aligned}$$

For $s \geq 3$, the claim is shown by means of Proposition 3.11:

$$\begin{aligned}\frac{d\left(\psi_H^s \star u\right)}{dx}(x) &= \left(\frac{d\psi_H^s}{dx} \star u\right)(x) \\ &\overset{(3.11)}{=} \left(\partial_H \psi_H^{s-1} \star u\right)(x) \\ &= \left(\psi_H^{s-1} \star \partial_H u\right)(x), \qquad \forall x\in\mathbb{R}, \qquad \forall H>0.\end{aligned}$$

Now that the claim has been shown for $\alpha = 1$, the proof is completed by repetitive application of the result for $\alpha = 1$. ∎

3.4 Central spline filtering

Now that the central B-splines are defined, they can be used to construct central spline filters, which form the subject of this section.

A central spline filter convolves the function to be filtered against a central spline kernel that is a linear combination of central B-splines (Definition 3.13, Proposition 3.14). A well-known example of such a kernel is the symmetric central spline kernel, which has symmetrically distributed integer nodes (Example 3.15, Figure 3.2). Another example is the one-sided central spline kernel, which differs from the symmetric central spline kernel in that its (integer) nodes and are chosen such that the kernel support is located on *one side* of the origin (Example 3.16, Figure 3.3). A variant of this kernel is the shifted one-sided kernel, whose support is shifted towards the origin as far as possible (Remark 3.17, Figure 3.4).

An important property of a central spline kernel is that it reproduces polynomials up to a certain degree ($2r-1$ for symmetric kernels and $2r-2$ in general, with r as in Definition 3.13), i.e. the convolution of the kernel with such a polynomial is equal to that polynomial itself (Proposition 3.18, Proposition 3.19). This property plays an important role in the convergence analysis in the next chapter.

The application of a central spline filter to a DG approximation is useful for four reasons. One: the filter works as a smoothing operator in the following manner. In general, the convolution of two functions is differentiable at least as many times as the sum of the differentiability orders of the individual functions. As a consequence, the order of differentiability of the unfiltered function is increased by at least the order of differentiability of the applied central B-splines (i.e. $s-2$). This smootness-increasing property can be used to tackle the problematic effect of the discontinuous nature of DG approximations along element boundaries on streamline visualisation techniques (cf. Section 2.4).

Two: the filter can be used to extract derivatives of the solution (cf. Theorem 4.17 in the next chapter). One of the research questions is whether it is possible to use this information in an (implicit) ODE scheme that is particularly useful for streamline visualisation.

Three: the computational costs of the filtering of a DG approximation are relatively low for two reasons. First of all, the filter needs to be applied only once, at the final time. Moreover, a central spline kernel has compact support, so the convolution can be computed with the help of small matrix-vector multiplications.

Four: although a central spline filter is independent of the underlying physics and numerics, it can be shown that, for a certain class of problems, the convergence rate of the DG approximation is at least preserved by the filter. This convergence-conserving property is obtained in the next chepter (cf. Theorem 4.17).

The next section confirms the smoothness-increasing convergence-conserving nature of central spline filters by means of a one-dimensional periodic linear example.

Definition 3.13 (Central spline kernel)
A *central spline kernel* $K^{s,\sigma,\{q_1,\ldots,q_{2r-1}\}}$, where $s,\sigma,r\in\mathbb{N}_1$ and where $q_1,\ldots,q_{2r-1}\in\mathbb{R}$ are distinct real nodes, is a linear combination of central B-splines (Definition 3.7) of the form:

$$K^{s,\sigma,\{q_1,\ldots,q_{2r-1}\}}(x)=\sum_{j=1}^{2r-1}\gamma_j^{\sigma,\{q_1,\ldots,q_{2r-1}\}}\psi^s\left(x-q_j\right),\qquad\forall x\in\mathbb{R},\tag{3.13}$$

where the coefficients $\gamma_j^{\sigma,\{q_1,\ldots,q_{2r-1}\}}$ are the unique solution (cf. Proposition 3.14 below) to the linear system:

$$\sum_{j=1}^{2r-1}\gamma_j^{\sigma,\{q_1,\ldots,q_{2r-1}\}}\int_{\mathbb{R}}\psi^\sigma(\xi)(\xi+q_j)^m\,\mathrm{d}\xi=\begin{cases}1, & \text{for } m=0,\\ 0, & \text{for all } m=1,\ldots,2r-2.\end{cases}\tag{3.14}$$

Note that the matrix coefficients can be easily obtained by applying (the binomial theorem and) Peano's theorem (Theorem 3.3). In the remainder of this report, the following notation will be tacitly assumed:

$$K_H^{s,\sigma,\{q_1,\ldots,q_{2r-1}\}}(x):=\frac{1}{H}K^{s,\sigma,\{q_1,\ldots,q_{2r-1}\}}\left(\frac{x}{H}\right),\qquad\forall x\in\mathbb{R},\qquad\forall H>0.$$

See also [BS77, p. 98-101] and [CLSS03, p. 583,584]. ⌟

Proposition 3.14 (Existence and uniqueness of the kernel coefficients)
The system (3.14) is a non-singular linear system. Hence, the existence and uniqueness of the kernel coefficients is guaranteed.

Proof:
See also [BS76, Lemma 8.1]. First, define

$$p_m(q):=\int_{\mathbb{R}}\psi^\sigma(\xi)(\xi+q)^m\,\mathrm{d}\xi,\qquad\forall m=0,\ldots,2r-2,$$

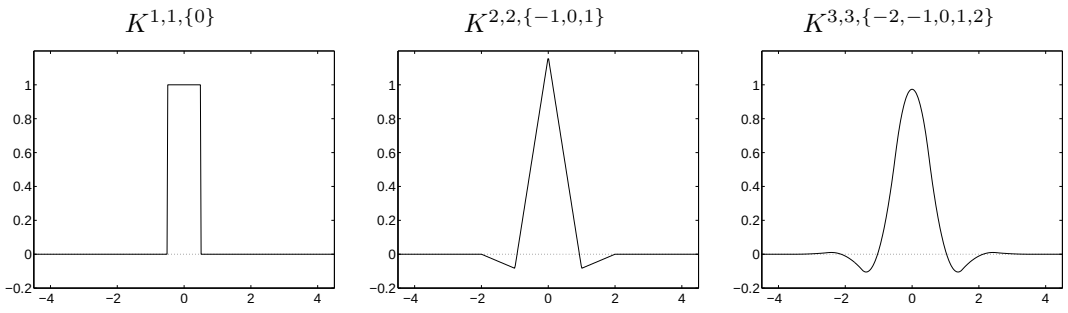

Figure 3.2: Symmetric central spline kernels (Example 3.15): notice that, as the order increases, the support and the smoothness of the symmetric central spline kernels increase.

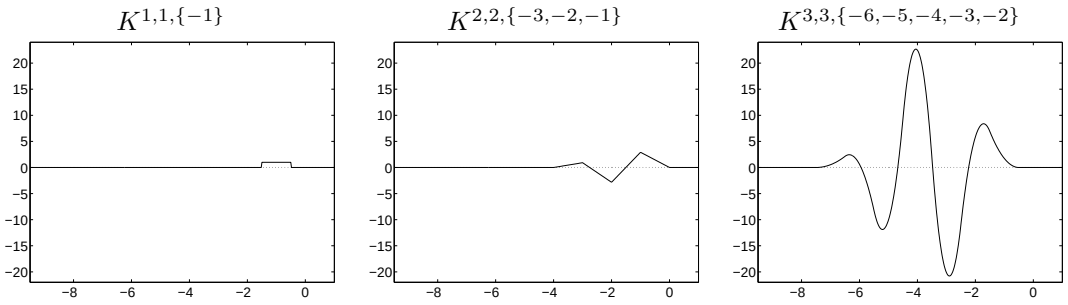

Figure 3.3: One-sided central spline kernels (Example 3.16): unlike symmetric kernels, one-sided kernels have a support that is located on *one side* of the origin.

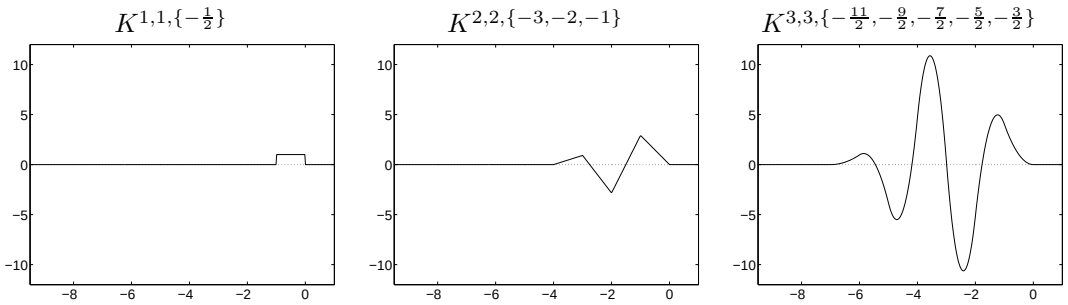

Figure 3.4: Shifted one-sided central spline kernels (Remark 3.17): unlike the 'ordinary' one-sided kernel, the shifted one-sided kernel has a support that is shifted towards the origin as far as possible.

and observe that $p_m(q)$ is a monic polynomial of degree m, as the integral over a B-spline is equal to 1 (cf. (3.4)). In other words, $p_m(q)$ is of the form:

$$p_m(q) = x^m + \sum_{\ell=0}^{m-1} \lambda_{m,\ell}\, x^\ell, \qquad \forall m = 0, ..., 2r-2. \tag{3.15}$$

As a consequence, the matrix corresponding to the system (3.14) can also be written as follows:

$$[p_m(q_j)]_{m=0,...,2r-2,\, j=1,...,2r-1} \in \mathbb{R}^{(2r-1)\times(2r-1)}.$$

That this system has linearly independent row vectors can be shown by means of reductio ad absurdum. Suppose the contrary, i.e. suppose there exists $M \in \{0, ..., 2r-2\}$ such that row M is a linear combination of the other rows. This implies that there exist constants $\{C_m\}_{m=0,...,2r-2}$, with $C_M = 0$, such that:

$$p_M(q_j) = \sum_{m=0}^{2r-2} C_m\, p_m(q_j), \qquad \forall j = 1, ..., 2r-1.$$

this can be rewritten using (3.15):

$$q_j^M + \sum_{\ell=0}^{M-1} \lambda_{M,\ell}\, q_j^\ell = \sum_{m=0}^{2r-2} C_m \left(q_j^m + \sum_{\ell=0}^{m-1} \lambda_{m,\ell}\, q_j^\ell \right), \qquad \forall j = 1, ..., 2r-1.$$

Reordering gives:

$$q_j^M + \sum_{\ell=0}^{M-1} \lambda_{M,\ell}\, q_j^\ell = \sum_{\ell=0}^{2r-2} \left(C_\ell + \sum_{m=\ell+1}^{2r-2} C_m \lambda_{m,\ell} \right) q_j^\ell, \qquad \forall j = 1, ..., 2r-1.$$

Bringing all terms to one side yields:

$$\begin{aligned}
&\sum_{\ell=0}^{M-1} \underbrace{\left(C_\ell + \sum_{m=\ell+1}^{2r-2} C_m \lambda_{m,\ell} - \lambda_{M,\ell} \right)}_{=0} q_j^\ell \\
&+ \underbrace{\left(C_M + \sum_{m=M+1}^{2r-2} C_m \lambda_{m,M} - 1 \right)}_{=0} q_j^M \\
&+ \sum_{\ell=M+1}^{2r-2} \underbrace{\left(C_\ell + \sum_{m=\ell+1}^{2r-2} C_m \lambda_{m,\ell} \right)}_{=0} q_j^\ell = 0, \qquad \forall j = 1, ..., 2r-1.
\end{aligned}$$

Since the nodes $q_1, ..., q_{2r-1}$ are distinct reals, this polynomial of degree $2r-2$ in the variable q_j has more roots than its degree. Hence, all of the coefficients must be equal to zero, as indicated in the equation above. This implies that

$$\begin{aligned}
0 &= C_{2r-2}, \\
0 &= C_{2r-3} + C_{2r-2}\lambda_{2r-2,2r-3} = C_{2r-3}, \\
&\vdots \\
0 &= C_{M+1} + \sum_{m=M+2}^{2r-2} \underbrace{C_m}_{=0} \lambda_{m,M+1} = C_{M+1}, \\
0 &= \underbrace{C_M}_{=0} + \sum_{m=M+1}^{2r-2} \underbrace{C_m}_{=0} \lambda_{m,M} - 1 = -1.
\end{aligned}$$

Since a contradiction has been found, the original assumption must be false. As a consequence, the system (3.14) has independent rows and must be non-singular. ∎

Example 3.15 (Symmetric central spline kernel)
The central spline kernel (Definition 3.13) $K^{s,\sigma,\{q_j=-r+j\}_{j=1,\dots,2r-1}}$ is also known as the *symmetric central spline kernel*.For $s,\sigma,r=1$, the system (3.14) is trivial, and the symmeric central spline kernel reads:

$$K^{1,1,\{0\}}(x)=\psi^1(x)\,.$$

For $s,\sigma,r=2$, the system reads:

$$\begin{bmatrix} 1 & 1 & 1 \\ 1 & 0 & -1 \\ \frac{7}{6} & \frac{1}{6} & \frac{7}{6} \end{bmatrix}\begin{bmatrix} \gamma_1^{2,\{-1,0,1\}} \\ \gamma_2^{2,\{-1,0,1\}} \\ \gamma_3^{2,\{-1,0,1\}} \end{bmatrix}=\begin{bmatrix} 1 \\ 0 \\ 0 \end{bmatrix} \qquad \Rightarrow \qquad \begin{bmatrix} \gamma_1^{2,\{-1,0,1\}} \\ \gamma_2^{2,\{-1,0,1\}} \\ \gamma_3^{2,\{-1,0,1\}} \end{bmatrix}=\begin{bmatrix} -\frac{1}{12} \\ \frac{7}{6} \\ -\frac{1}{12} \end{bmatrix}.$$

Substitution of these coeffcients into (3.13) yields the following symmetric central kernel:

$$K^{2,2,\{-1,0,1\}}(x)=-\frac{1}{12}\psi^2(x+1)+\frac{7}{6}\psi^2(x)-\frac{1}{12}\psi^2(x-1)\,.$$

For an illustration, see Figure 3.2. ⌟

Example 3.16 (One-sided central spline kernel)
The central spline kernel (Definition 3.13) $K^{s,\sigma,\{q_j=\left\lfloor -(2r-1)-\frac{s}{2}\right\rfloor+j\}_{j=1,\dots,2r-1}}$ is also known as the *one-sided central spline kernel*.For $s,\sigma,r=1$, the system (3.14) is trivial, and the one-sided central spline kernel reads:

$$K^{1,\{-1\}}(x)=\psi^1(x+1)\,.$$

For $s,\sigma,r=2$, the system reads:

$$\begin{bmatrix} 1 & 1 & 1 \\ 3 & 2 & 1 \\ \frac{55}{6} & \frac{25}{6} & \frac{7}{6} \end{bmatrix}\begin{bmatrix} \gamma_1^{2,\{-3,-2,-1\}} \\ \gamma_2^{2,\{-3,-2,-1\}} \\ \gamma_3^{2,\{-3,-2,-1\}} \end{bmatrix}=\begin{bmatrix} 1 \\ 0 \\ 0 \end{bmatrix} \qquad \Rightarrow \qquad \begin{bmatrix} \gamma_1^{2,\{-3,-2,-1\}} \\ \gamma_2^{2,\{-3,-2,-1\}} \\ \gamma_3^{2,\{-3,-2,-1\}} \end{bmatrix}=\begin{bmatrix} \frac{11}{12} \\ -\frac{17}{6} \\ \frac{35}{12} \end{bmatrix}.$$

After solving for the coefficients, the following one-sided central spline kernel is obtained:

$$K^{2,\{-3,-2,-1\}}(x)=\frac{11}{12}\psi^2(x+3)-\frac{17}{6}\psi^2(x+2)+\frac{35}{12}\psi^2(x+1)\,.$$

For an illustration, see Figure 3.3. ⌟

Remark 3.17 (Shifted one-sided central spline kernel)
Note that the support of the one-sided central spline kernel (Example 3.16) is not as close to the origin as possible, for odd values of r. Alternatively, one could use the following nodes, to ensure that support of the kernel is shifted to the origin as far as possible:

$$q_j=-(2r-1)-\frac{s}{2}+j, \qquad \forall j=1,...,2r-1.$$

See Figure 3.4 for an illustration. ⌟

Proposition 3.18 (Reproduction of polynomials)
The central spline kernel $K^{s,s,\{q_1,\dots,q_{2r-1}\}}$ (Definition 3.13) reproduces polynomials of degree $2r-2$ and lower in the sense that the convolution of the kernel with such a polynomial is equal to that polynomial itself:

$$K^{s,s,\{q_1,\dots,q_{2r-1}\}}\star p=p, \qquad \forall p\in\mathcal{P}^{2r-2}(\mathbb{R}).$$

PROOF:
In favour of notational brevity, omit the nodes in the notation in the kernel (coefficients) from here on. Using the functions $\{x^m\}_{m=0,...,2r-2}$ as basis for $\mathcal{P}^{2r-2}(\mathbb{R})$, it suffices to show that

$$\int_{\mathbb{R}} K^{s,s}(\xi)(x-\xi)^m \,\mathrm{d}\xi = \sum_{j=1}^{2r-1} \gamma_j^s \int_{\mathbb{R}} \psi^s(\xi - q_j)(x-\xi)^m \,\mathrm{d}\xi = x^m, \quad \forall m = 0, ..., 2r-2. \tag{3.16}$$

For $m = 0$, (3.16) follows immediately from (3.14) for $m = 0$:

$$\sum_{j=1}^{2r-1} \gamma_j^s \int_{\mathbb{R}} \psi^s(\xi - q_j) \,\mathrm{d}\xi = 1.$$

For $m = 1, ..., 2r-2$, the claim is shown with the help of induction. Suppose that (3.16) is satisfied up to $m-1$. As a consequence,

$$\begin{aligned}\int_{\mathbb{R}} K^{s,s}(\xi)(x-\xi)^m \,\mathrm{d}\xi &= \sum_{j=1}^{2r-1} \gamma_j^s \int_{\mathbb{R}} \psi^s(\xi - q_j)(x-\xi)^m \,\mathrm{d}\xi \\ &= \underbrace{\left(\sum_{j=1}^{2r-1} \gamma_j^s \int_{\mathbb{R}} \psi^s(\xi - q_j)(x-\xi)^{m-1} \,\mathrm{d}\xi \right)}_{=x^{m-1}} x \\ &\quad - \sum_{j=1}^{2r-1} \gamma_j^s \int_{\mathbb{R}} \psi^s(\xi - q_j)(x-\xi)^{m-1} \xi \,\mathrm{d}\xi.\end{aligned}$$

Use (3.16) for $m-1$:

$$\int_{\mathbb{R}} K^{s,s}(\xi)(x-\xi)^m \,\mathrm{d}\xi = x^m - \sum_{j=1}^{2r-1} \gamma_j^s \int_{\mathbb{R}} \psi^s(\xi - q_j)(x-\xi)^{m-1} \xi \,\mathrm{d}\xi.$$

Define $\xi' = -\xi$:

$$\int_{\mathbb{R}} K^{s,s}(\xi)(x-\xi)^m \,\mathrm{d}\xi = x^m - \sum_{j=1}^{2r-1} \gamma_j^s \int_{\mathbb{R}} \psi^s(-\xi' - q_j)(x+\xi')^{m-1} \xi' \,\mathrm{d}\xi'.$$

Using the binomial theorem:

$$\int_{\mathbb{R}} K^{s,s}(\xi)(x-\xi)^m \,\mathrm{d}\xi = x^m - \sum_{\ell=0}^{m-1} \frac{(m-1)!}{\ell!(m-1-\ell)!} x^{m-1-\ell} \sum_{j=1}^{2r-1} \gamma_j^s \int_{\mathbb{R}} \psi^s(-\xi' - q_j) \xi'^{\ell+1} \,\mathrm{d}\xi'.$$

Define $\xi'' = \xi' + q_j$ and use the fact that a central B-spline is an even function (cf. Proposition 3.9):

$$\int_{\mathbb{R}} K^{s,s}(\xi)(x-\xi)^m \,\mathrm{d}\xi = x^m - \sum_{\ell=0}^{m-1} \frac{(m-1)!}{\ell!(m-1-\ell)!} x^{m-1-\ell} \sum_{j=1}^{2r-1} \gamma_j^s \int_{\mathbb{R}} \psi^s(\xi'')(\xi'' + q_j)^{\ell+1} \,\mathrm{d}\xi''.$$

Applying (3.14) ends the proof. ∎

Proposition 3.19 (Reproduction of polynomials in the symmetric case)
The symmetric central spline kernel $K^{s,s,\{q_j=-r+j\}_{j=1,...,2r-1}}$ (Example 3.15) reproduces polynomials of degree $2r-1$ or lower in the sense that the convolution of the kernel with such a polynomial is equal to that polynomial itself:

$$K^{s,s,\{q_j=-r+j\}_{j=1,...,2r-1}} \star p = p, \qquad \forall p \in \mathcal{P}^{2r-1}(\mathbb{R}).$$

PROOF:
With the help of the binomial theorem and the symmetry of the nodes it can be shown that

$$\sum_{j=1}^{2r-1} \gamma_j^{s,\{q_j=-r+j\}_{j=1,\dots,2r-1}} \int_{\mathbb{R}} \psi^s(\xi'')(\xi''+q_j)^{2r-1}\,\mathrm{d}\xi'' = 0.$$

Using this result, the claim is obtained by following the proof of Proposition 3.18. ∎

3.5 Central spline filtering of the DG approximation for a one-dimensional linear periodic problem

The previous section introduced central spline kernels to enhance the smoothness while conserving the convergence. This section discusses some computational aspects and the performance for a one-dimensional periodic linear problem.

To compute the filtered DG approximation for such a problem, the convolution with the central spline kernel is rewritten as a linear combination of convolutions with central B-splines (Example 3.20). An illustration of the performance of the symmetric and the one-sided central spline filter for this problem at the initial time can be found in Figure 3.5 and Figure 3.6. The large improvement in the convergence rate is due to the fact that the underlying mesh is equidistant [CLSS03, p. 585, 590]. Furthermore, Figure 3.6 emphasizes that improvement/conservation of the convergence rate does *not* necessarily lead to improvement/conservation of the absolute error. Nevertheless, both figures confirm the theory that the smoothness is enhanced, regardless of the filtering type or the underlying DG approximation (cf. Section 3.4).

Figure 3.7 illustrates the performance of the symmetric central spline filter for the same problem at time $t = 2\pi$. The effect of time-stepping errors on the convergence rate of the filtered DG approximation becomes clear by comparing this figure to Figure 3.5. It should be noted that the convergence analysis in present literature relies on exact time integration. Thus, current theory on the convergence rate is no longer valid once a discrete time-stepping scheme is used in the DG approximation. However, as before, this should and indeed does not effect the smoothness of the filtered DG approximation.

Altogether, the test cases in this section confirm the smoothness-increasing convergence-conserving properties of central spline filters. The next section considers the consequences of the smoothing effect of central spline filtering for streamline visualisation.

Example 3.20 (Computational aspects)
Consider Example 2.8 for an equidistant mesh with constant element width h. Let $u_h \in \mathcal{P}^k_{\mathcal{X}_h}(X)$ denote the DG approximation at a certain time. Its (weak) derivative of order $\alpha \in \mathbb{N}_0$ can be filtered with the help of the central spline kernel $K_h^{s,s+\alpha,\{q_1,\dots,q_{2r-1}\}}$ (Definition 3.13, and Theorem 4.17 in the next chapter). Here, it will be assumed that the nodes $q_1 < \dots < q_{2r-1}$ take subsequent integer values. For $x \in X_q$ with $q \in I$, the filtered derivative $(D^\alpha u_h)^\star$ is obtained as follows (in favour of notational brevity, the nodes $\{q_1, \dots, q_{2r-1}\}$ are omitted in the notation of the kernel (coefficients) from here on):

$$(D^\alpha u_h)^\star(x) = \left(K_h^{s,s+\alpha} \star \partial_h^\alpha u_h\right)(x) = \left(\partial_h^\alpha K_h^{s,s+\alpha} \star u_h\right)(x)$$

Expand the central difference quotient:

$$\begin{aligned}(D^\alpha u_h)^\star(x) = &\sum_{J=0}^{\alpha} \frac{1}{h^\alpha}(-1)^J \frac{\alpha!}{(\alpha-J)!J!} \\ &\int_{\mathbb{R}} K_h^{s,s+\alpha}\left(x + \left(\frac{\alpha}{2} - J\right)h - \xi\right) u_h(\xi)\,\mathrm{d}\xi.\end{aligned}$$

Next, exploit the fact that the support of the integrand is contained in a finite number of elements (whenever information outside the domain is required, the periodic boundary conditions should

actually be taken into account, which is not included in the notation here for the sake of simplicity):

$$(D^\alpha u_h)^\star(x) = \sum_{J=0}^{\alpha} \sum_{j=q_{a_J}:=q+\left\lfloor \frac{\alpha}{2}-J \right\rfloor - \left\lceil q_{2r-1}+\frac{s}{2} \right\rceil}^{q_{b_J}:=q+\left\lceil \frac{\alpha}{2}-J \right\rceil - \left\lfloor q_1-\frac{s}{2} \right\rfloor} \frac{1}{h^\alpha}(-1)^J \frac{\alpha!}{(\alpha-J)!J!} \int_{X_j} K_h^{s,s+\alpha}\left(x+\left(\frac{\alpha}{2}-J\right)h-\xi\right) u_h^j(\xi)\,\mathrm{d}\xi.$$

Switch to the unscaled kernel:

$$(D^\alpha u_h)^\star(x) = \sum_{J=0}^{\alpha} \sum_{j=q_{a_J}}^{q_{b_J}} \frac{1}{h^{\alpha+1}}(-1)^J \frac{\alpha!}{(\alpha-J)!J!} \int_{X_j} K^{s,s+\alpha}\left(\frac{x+\left(\frac{\alpha}{2}-J\right)h-\xi}{h}\right) u_h^j(\xi)\,\mathrm{d}\xi.$$

Write the DG solution as a linear combination of monomials (cf. (2.9)) and the kernel as a linear combination of B-splines (cf. (3.13)):

$$(D^\alpha u_h)^\star(x) = \sum_{J=0}^{\alpha} \sum_{j=q_{a_J}}^{q_{b_J}} \sum_{\ell=0}^{k} \sum_{m=1}^{2r-1} \frac{1}{h^{\alpha+1}}(-1)^J \frac{\alpha!}{(\alpha-J)!J!} C^{j,\ell}\gamma_m^{s+\alpha} \int_{X_j} \psi^s\left(\frac{x+\left(\frac{\alpha}{2}-J\right)h-\xi}{h}-q_m\right)\left(\frac{\xi-\frac{x_{j-\frac{1}{2}}+x_{j+\frac{1}{2}}}{2}}{h}\right)^\ell \mathrm{d}\xi$$

Define $\xi' = \frac{\xi-x-\left(\frac{\alpha}{2}-J\right)h}{h}+q_m$, apply a change of variables, and use the symmetry of the B-splines:

$$(D^\alpha u_h)^\star(x) = \sum_{J=0}^{\alpha} \sum_{j=q_{a_J}}^{q_{b_J}} \sum_{\ell=0}^{k} \sum_{m=1}^{2r-1} \frac{1}{h^\alpha}(-1)^J \frac{\alpha!}{(\alpha-J)!J!} C^{j,\ell}\gamma_m^{s+\alpha} \int_{\frac{1}{h}(x_{j-\frac{1}{2}}-x-\left(\frac{\alpha}{2}-J\right)h)+q_m}^{\frac{1}{h}(x_{j+\frac{1}{2}}-x-\left(\frac{\alpha}{2}-J\right)h)+q_m} \psi^s(\xi')\left(\xi'-q_m+\frac{x+\left(\frac{\alpha}{2}-J\right)h-\frac{x_{j-\frac{1}{2}}+x_{j+\frac{1}{2}}}{2}}{h}\right)^\ell \mathrm{d}\xi'$$

The integral in this last expression can be computed exactly, e.g. with the help of Gaussian quadrature. ⌟

3.6 Consequences for streamline visualisation

The previous section illustrated the smoothness-increasing convergence-conserving nature of central spline filters. Now, it is time to consider the consequences for streamline visualisation.

Steffen et al. [SCKR08, Section 6] have applied a two-dimensional symmetric central spline filter to a DG approximation of a vector field, prior to the ODE solver that computes the corresponding streamlines. They observed both a reduction in the costs of the streamline visualisation and an error improvement (Figure 3.8). However, there are also two drawbacks of their approach. The first is that the current multi-dimensional central spline filters are only applicable for quadrilateral meshes. It is one of the main goals of this research to make the filters suitable for triangular meshes. The second is that the symmetric filter cannot be applied near the boundary of the spatial domain.

The one-sided kernel provides options to tackle both these issues. First of all, unlike the symmetric filter, the one-sided filter can enhance the accuracy of streamline visualisation techniques

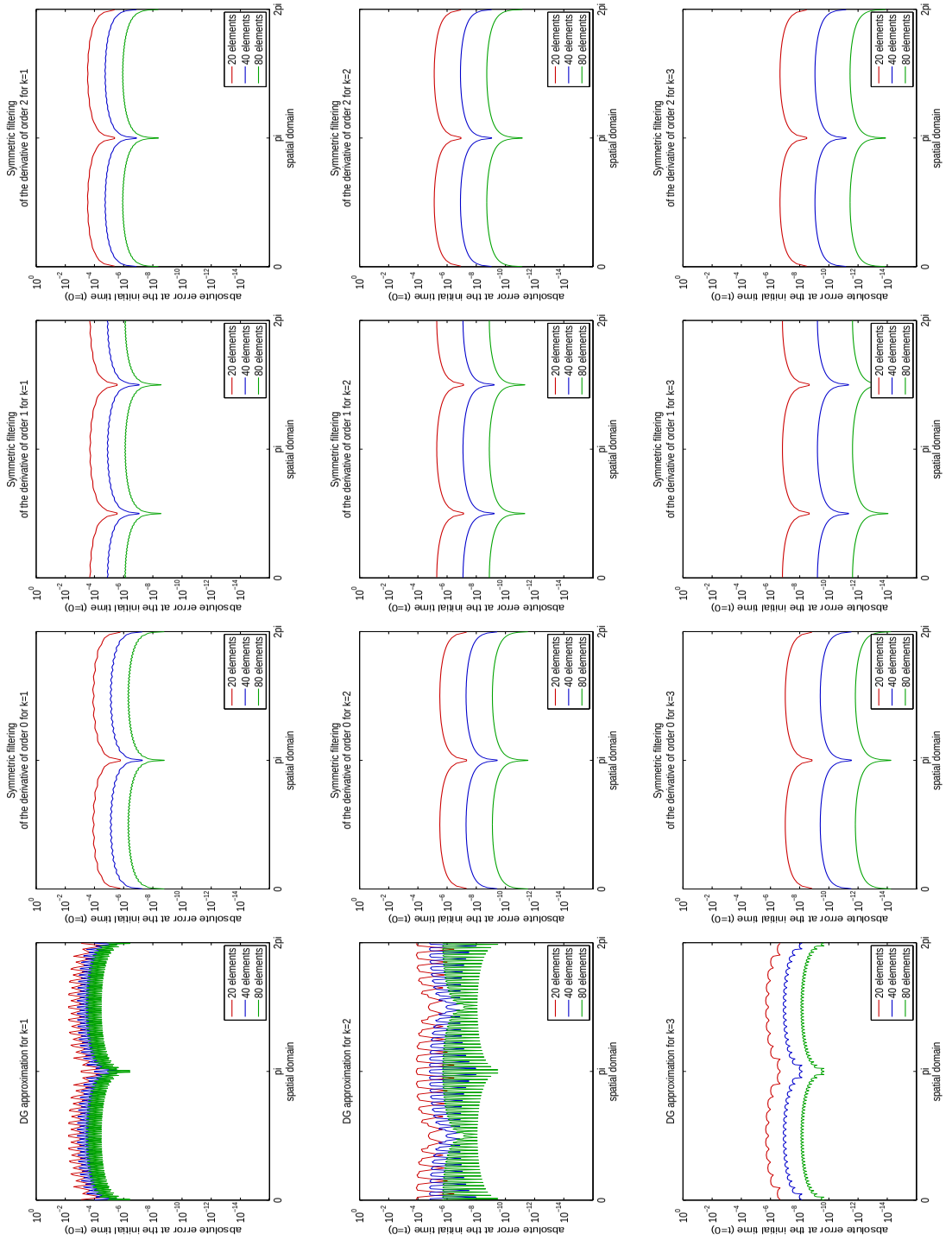

Figure 3.5: Absolute value of the error in the DG approximation after application of the symmetric central spline filter $\left|D^{\alpha}u - (D^{\alpha}u_h)^{\star}\right|$ for a one-dimensional periodic linear hyperbolic problem with velocity $c = 1$ at the initial time (Example 2.9, Example 3.20, Example 3.15). The initial condition is the sine function. Notice that the filter increases both the convergence rate and the smoothness. In this case, the filtered error is smaller than the unfiltered error in all cases.

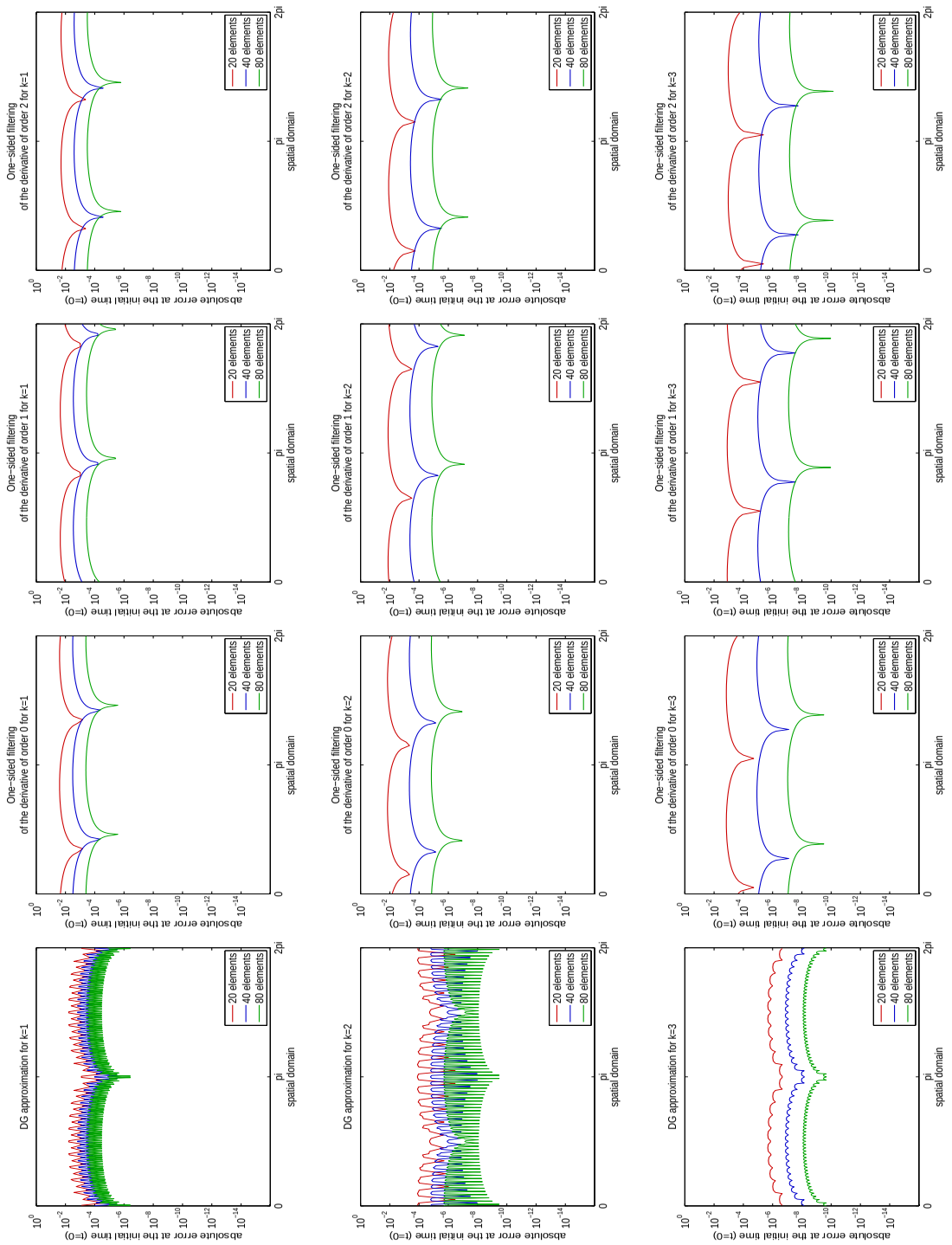

Figure 3.6: Absolute value of the error in the DG approximation after application of the one-sided central spline filter $\left|D^{\alpha}u - (D^{\alpha}u_h)^{\star}\right|$ for a one-dimensional periodic linear hyperbolic problem with velocity $c = 1$ at the initial time (Example 2.9, Example 3.20, Example 3.16). The initial condition is the sine function. Notice that the filter increases both the convergence rate and the smoothness, but not necesarily the absolute error. So the absolute filtered errors are worse for coarse meshes, but the convergence rate is at least preserved and even improved in this case.

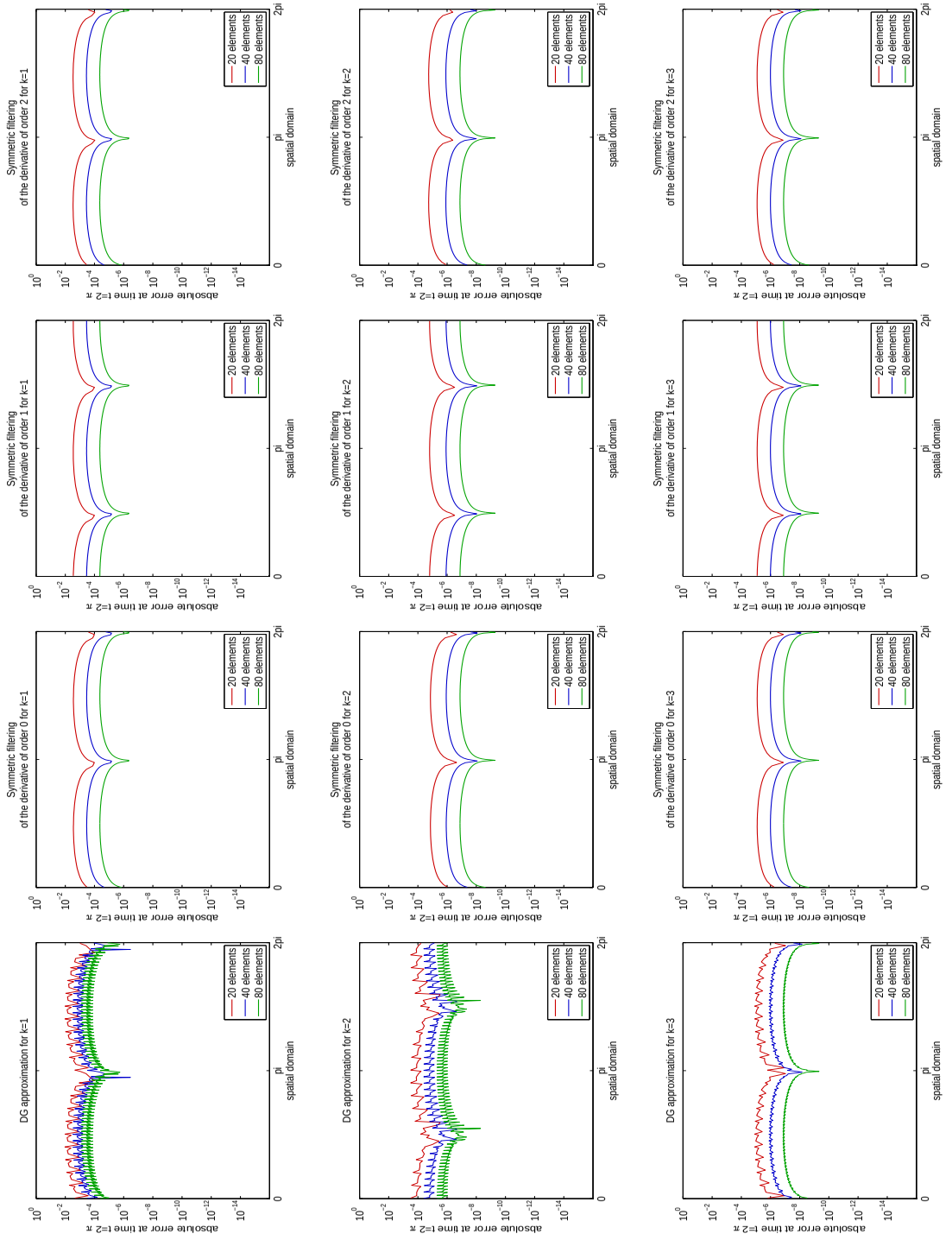

Figure 3.7: Absolute value of the error in the DG approximation after application of the symmetric central spline filter $\left|D^{\alpha}u - (D^{\alpha}u_h)^{\star}\right|$ for a one-dimensional periodic linear hyperbolic problem with velocity $c = 1$ at time $t = 2\pi$ (Example 2.9, Example 3.20, Example 3.15). The initial condition is the sine function and the time step equals $0.1h$. Notice that the increase of the convergence rate is smaller than for the initial time, but the enhancement of the smoothness is the similar.

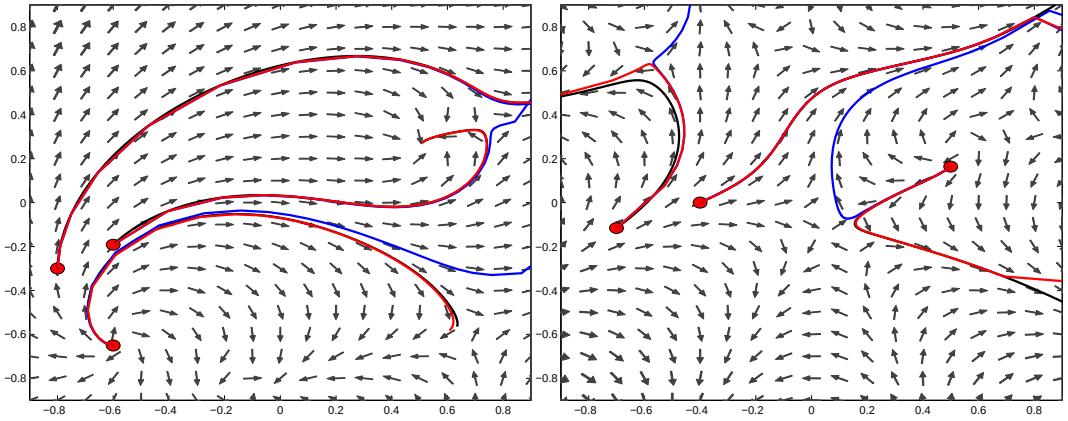

Figure 3.8: Enhancement of streamline accuracy through two-dimensional symmetric central spline filtering as published in [SCKR08]: The arrows display the directional field of the underlying vector field. The plot shows exact streamlines of the original vector field (black lines under red lines), streamlines of the $\mathcal{L}^2$-projected field (blue lines under red lines), and streamlines of the $\mathcal{L}^2$-projected field after filtering (red lines). The seeding points of the streamlines are indicated by circles. All streamlines were calculated using RK-4/5 with an error tolerance of 10^{-6}. Observe that the main differences in the computations occur near critical points. For more details, see [SCKR08].

in a backward one-dimensional manner along the streamline, as was proposed by Walfish et al. [WRKH09]. Note that the symmetric central spline kernel would be practically unsuitable for this approach: it would require points on the streamline that are yet to be computed with the ODE solver. This issue is illustrated in Figure 3.9. Nevertheless, this alternative approach introduces new difficulties. First of all, in order to filter along the streamline, the known discrete data on the streamline need to be interpolated in order to compute the convolution. The effect of the corresponding error on the filtering is currently unknown. Furthermore, it is not certain that the error estimations for a one-dimensional central spline filter remain valid along an arbitrary curve in a two-dimensional domain.

Second of all, unlike the symmetric filter, the one-sided filter can be applied near boundaries. Unfortunately, this leads to new difficulty: the one-sided filter is inconsistent with Dirichlet boundary conditions in the sense that the filtered boundary value is generally not equal to the unfiltered boundary value. To illustrate the seriousness of this issue, consider the velocity profile around an airfoil. At the surface of the airfoil, the velocity perpendicular to the surface must be equal to zero. If the filter does not respect this boundary condition, a streamline that is computed from the filtered DG approximation might go through the boundary, which is physically impossible. The question is whether it is possible to construct a spline filtering strategy that is consistent with the boundary conditions. Most likely, this will require the use of different kernels throughout the domain that converge to a Dirac distribution towards the boundary of the domain. A non-smooth variation in the kernels could introduce non-smoothness in the filtered solution (cf. [RSA05, Figure 4.2]).

Altogether, this research will mainly focus on a spline filtering stratey that is consistent with the boundary conditions, and that can be applied for triangular meshes.

3.7 Conclusion

The lack of smoothness of a DG approximation can hamper its visualisation in the form of streamlines. This problem can be tackled through central spline filtering. A central spline filter convolves the function to be filtered against a central spline kernel, which is a linear combination of central

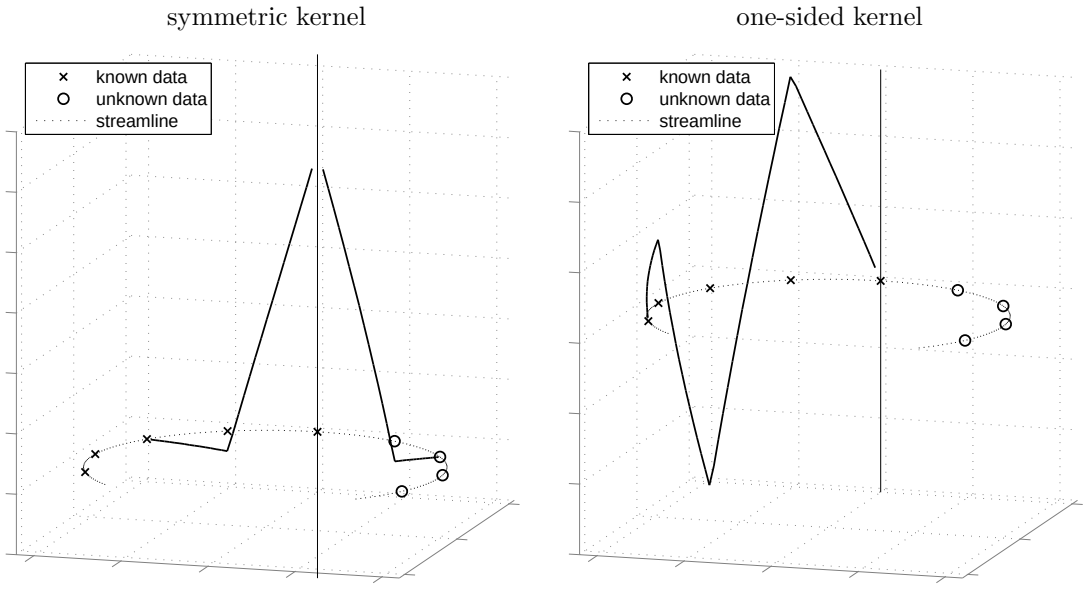

Figure 3.9: The one-sided central spline filter can enhance the accuracy of streamline visualisation techniques with a one-dimensional approach. The symmetric filter would require unknown data.

B-splines. The filter enhances the smoothness in the sense that the filtered solution is at least differentiable up to the order of the central B-splines minus two. This benefits the accuracy of streamline visualisation. Additionally, a reduction of oscillations in the error is observed. Unfortunately, present spline filters can only be applied for quadrilateral meshes, and are either not applicable near the boundary or inconsistent with the boundary conditions. This research seeks to overcome these difficulties.

Chapter 4

Conserving the convergence

4.1 Introduction

The previous chapter introduced smoothness-increasing convergence-conserving central spline filters to improve the accuracy of streamline visualisations of DG approximations. This chapter proves the fact that these filters are indeed convergence-conserving for a certain class of problems. It provides a (derivative) error estimation for DG approximations based on the first-order upwind flux and exact time integration on one-dimensional non-equidistant meshes for periodic linear hyperbolic equations with a sufficiently smooth exact solution. A more general result that also applies for multi-dimensional quadrilateral meshes has been shown by Cockburn et al. in [CLSS03].

The derivation of the error estimate makes use of (negative-order) Sobolev norms and the Brambe-Hilbert Lemma (Section 4.2). After an intermediate (derivative) error estimation for an arbitrary filtered $\mathcal{L}^2$-function has been given (Section 4.3), the estimation can be refined by making use of the characteristics of the DG scheme under consideration (Section 4.4). Finally, a conclusion is given (Section 4.5).

4.2 Auxiliary theory

Both the intermediate error estimation for arbitrary filtered $\mathcal{L}^2$-functions and the final error estimation for filtered DG approximations, which are discussed in the next two sections, make use of properties of (negative-order) Sobolev norms and the Bramble-Hilbert Lemma. Therefore, this auxiliary theory is discussed first in this section.

The derivation often makes use of the possibilty to switch between different types of (negative-order) Sobolev norms (Proposition 4.2). Moreover, it applies an estimation of the $\mathcal{L}^2$-norm of a smooth function in terms of sums of negative-order norms of derivatives of that function (Lemma 4.3).

The derivation also uses the Bramble-Hilbert Lemma (Lemma 4.4), which implies a convenient estimation for a certain class of bounded linear functionals that are zero when evaluated in a polynomial of sufficiently low degree (Proposition 4.5). This implication can be used to estimate the error in (piecewise) polynomial projections (Proposition 4.6, Corollary 4.7). Furthermore, it will be used in the next section to exploit the fact that a central spline kernel reproduces polynomials up to a certain degree.

Now that certain properties of Sobolev norms and the Bramble-Hilbert Lemma and its consequences have been discussed, these elements can be applied to obtain the error estimations in the next two sections.

Notation 4.1 ((Negative-order) Sobolev norms)
Consider Notation 2.1. For any domain $X \subseteq R$, consider the Sobolev norm:

$$\|u\|_{q,X} = \left(\sum_{j=0}^{q} \int_X \left| D^j u(x) \right|^2 \mathrm{d}x \right)^{\frac{1}{2}}, \qquad \forall u \in \mathcal{W}^{q,2}(X), \qquad \forall q \in \mathbb{N}_0.$$

Here, Dv denotes the weak derivative of v. Moreover, for any *open* domain $X \subseteq R$, define the negative-order Sobolev norm:

$$\|u\|_{-q,X} = \sup_{v \in \mathcal{C}_0^\infty(X)} \frac{\langle u, v \rangle_X}{\|v\|_{q,X}}, \qquad \forall u \in \mathcal{L}^2(X), \qquad \forall q \in \mathbb{N}_0.$$

Additionally, for all $H > 0$, and let ∂_H denote the central difference quotient (Notation 3.1). Finally, the symbol $\Subset$ should be interpreted to mean "is a subset of a compact subset of the interior of". ⌟

Proposition 4.2 (Switching between different types of Sobolev norms)
Consider Notation 4.1 and let $X_0 \subseteq X_1 \subseteq \mathbb{R}$. Then, for all $q \in \mathbb{N}_0$

$$\|u\|_{q,X_1} \leq \|u\|_{q+1,X_1}, \qquad \forall u \in \mathcal{W}^{q+1,2}(X_1), \tag{4.1}$$

$$\|u\|_{-q-1,X_1} \leq \|u\|_{-q,X_1}, \qquad \forall u \in \mathcal{L}^2(X_1), \qquad X_0, X_1 \text{ open}, \tag{4.2}$$

$$\|u\|_{q,X_0} \leq \|u\|_{q,X_1}, \qquad \forall u \in \mathcal{W}^{q,2}(X_1), \tag{4.3}$$

$$\|u\|_{-q,X_0} \leq \|u\|_{-q,X_1}, \qquad \forall u \in \mathcal{L}^2(X_1), \qquad X_0, X_1 \text{ open}. \tag{4.4}$$

Proof:
The first and third equation follow from the definition of the Sobolev norm. The second equation can be shown using the first:

$$\|u\|_{-q-1,X} = \sup_{v \in \mathcal{C}_0^\infty(X)} \frac{\langle u, v \rangle_X}{\|v\|_{q+1,X}} \leq \sup_{v \in \mathcal{C}_0^\infty(X)} \frac{\langle u, v \rangle_X}{\|v\|_{q,X}} = \|u\|_{-q,X}, \qquad \forall u \in \mathcal{L}^2(X), \qquad \forall q \in \mathbb{N}_0.$$

The fourth equation is obtained as follows:

$$\begin{aligned} \|u\|_{-q,X_0} &= \sup_{v \in \mathcal{C}_0^\infty(X_0)} \frac{\langle u, v \rangle_{X_0}}{\|v\|_{q,X_0}} = \sup_{\substack{v \in \mathcal{C}_0^\infty(X_1), \\ \mathrm{supp}(v) \Subset X_0}} \frac{\langle u, v \rangle_{X_1}}{\|v\|_{q,X_1}} \\ &\leq \sup_{v \in \mathcal{C}_0^\infty(X_1)} \frac{\langle u, v \rangle_{X_1}}{\|v\|_{q,X_1}} = \|u\|_{-q,X_1}, \qquad \forall u \in \mathcal{L}^2(X_1), \qquad \forall q \in \mathbb{N}_0, \end{aligned}$$

which completes the proof. ∎

Lemma 4.3 (Switching from the $\mathcal{L}^2$-norm to negative-order norm)
Consider Notation 4.1. Let $X_0 \Subset X_1 \subseteq \mathbb{R}$ with X_1 open and bounded. Furthermore, let $u \in \mathcal{W}^{q,2}(X_1)$. Then, for all $q \in \mathbb{N}_0$, there exists a constant $C > 0$ (independent of u) such that:

$$\|u\|_{0,X_0} \leq C \sum_{j=0}^{q} \left\| D^j u \right\|_{-q,X_1}.$$

Proof:
See [BS77, Lemma 4.2]. ∎

Lemma 4.4 (Bramble-Hilbert Lemma (special case))
Let $X \subseteq \mathbb{R}$ be an interval of length 1 and let $q \in \mathbb{N}_0$. Then,

$$\inf_{p \in \mathcal{P}^q(X)} \|u + p\|_{q+1,X} \leq C \left\| D^{q+1} u \right\|_{0,X}, \qquad \forall u \in \mathcal{W}^{q,2}(X),$$

for some constant $C > 0$ (independent of u).

PROOF:
A far more general result is shown in [BH70, Theorem 1] and [BH71, Theorem 1]. ∎

Proposition 4.5 (A consequence of the Bramble-Hilbert Lemma)
Let $q \in \mathbb{N}_0$. Furthermore, for all $x \in X_0 \subseteq \mathbb{R}$ and for all bounded intervals $X \subseteq \mathbb{R}$, consider a bounded linear functional $F_{x,X} : \mathcal{W}^{q+1,2}(X) \to \mathbb{R}$ such that

$$F_{x,X}(p) = 0, \qquad \forall p \in \mathcal{P}^q(X), \qquad \forall x \in X_0, \tag{4.5}$$

and

$$\sup_{x \in X_0} |F_{x,X}(u)| < \infty, \qquad \forall u \in \mathcal{W}^{q+1,2}(X). \tag{4.6}$$

Then,

$$|F_{x,X}(u)| \leq C\,|X|^{q+\frac{1}{2}} \left\|D^{q+1}u\right\|_{0,X}, \qquad \forall u \in \mathcal{W}^{q+1,2}(X), \qquad \forall x \in X_0.$$

for some constant $C > 0$ (independent of u, x, and X). Here, $|X|$ denotes the length of the interval X.
PROOF:
First, consider the case $X = [0,1]$. Because of (4.5),

$$\left|F_{x,[0,1]}(u)\right| = \inf_{p \in \mathcal{P}^q[0,1]} \left|F_{x,[0,1]}(u+p)\right|, \qquad \forall u \in \mathcal{W}^{q+1,2}[0,1], \qquad \forall x \in X_0.$$

By (4.6) and because $F_{x,[0,1]}$ is a bounded linear functional for all $x \in X_0$, the *principle of uniform boundedness* [Con85, p. 98] implies that there exists a constant $C > 0$ (independent of x and u) such that

$$\left|F_{x,[0,1]}(u)\right| \leq C\,\|u\|_{q+1,[0,1]}, \qquad \forall u \in \mathcal{W}^{q+1,2}[0,1], \qquad \forall x \in X_0.$$

Substitution yields:

$$\left|F_{x,[0,1]}(u)\right| \leq C \inf_{p \in \mathcal{P}^q[0,1]} \|u+p\|_{q+1,[0,1]}$$

Application of the Bramble-Hilbert Lemma (Lemma 4.4) now completes the proof for $X = [0,1]$. Next, consider arbitrary X. Let x_a denote the left endpoint of X. Moreover, for all $u \in \mathcal{W}^{q+1,2}(X)$, define $v_u \in \mathcal{W}^{q+1,2}[0,1]$ such that

$$u(x) = v_u\left(\frac{x - x_a}{|X|}\right), \qquad \forall x \in X.$$

Next, observe that

$$\begin{aligned}
|F_{x,X}(u)|^2 &= \left|F_{\frac{x-x_a}{|X|},[0,1]}(v_u)\right|^2 \\
&\leq C^2 \left\|D^{q+1}v_u\right\|^2_{0,[0,1]} \\
&= C^2 \int_0^1 \left|D^{q+1}v_u(\xi)\right|^2 \mathrm{d}\xi \\
&= C^2 \frac{1}{|X|} \int_{x_a}^{x_a+|X|} \left|\left(D^{q+1}v_u\right)\left(\frac{\xi - x_a}{|X|}\right)\right|^2 \mathrm{d}\xi \\
&= C^2\,|X|^{2q+1} \int_{x_a}^{x_a+|X|} \left|D^{q+1}\left(v_u\left(\frac{\xi - x_a}{|X|}\right)\right)\right|^2 \mathrm{d}\xi \\
&= C^2\,|X|^{2q+1} \int_{x_a}^{x_a+|X|} \left|D^{q+1}u\,(\xi)\right|^2 \mathrm{d}\xi \\
&= C^2\,|X|^{2q+1} \left\|D^{q+1}u\right\|^2_{0,X}, \qquad \forall u \in \mathcal{W}^{q+1,2}(X), \quad \forall x \in X.
\end{aligned}$$

Taking the square root completes the proof. ∎

Proposition 4.6 (Polynomial projection)
Consider Notation 2.6 and let $X_h = [x_a, x_a + h] \subseteq \mathbb{R}$ be a bounded interval of length $h > 0$. Furthermore, let $k \geq 0$. Then,

$$\left\|u - \mathbb{P}_{\mathcal{P}^k(X_h)} u\right\|_{0,X_h} \leq C h^{k+1} \left\|D^{k+1} u\right\|_{0,X_h}, \qquad \forall u \in \mathcal{W}^{k+1,2}(X_h),$$

for some constant $C > 0$ (independent of h and u).

Proof:
For all $x \in X_h$ and for all $h > 0$, define functionals $F_{x,X_h} : \mathcal{W}^{k+1,2}(X_h) \to \mathbb{R}$ such that

$$F_{x,X_h}(u) = \left(u - \mathbb{P}_{\mathcal{P}^k(X_h)} u\right)(x), \qquad \forall u \in \mathcal{W}^{k+1,2}(X_h), \qquad \forall x \in X_h.$$

Note that $|F_{x,X_h}(u)|$ is a continuous function of x on a bounded interval since any weakly differentiable function on a bounded domain can be identified with its continuous version [Eva98, p. 269]. Next, apply Proposition 4.5 to obtain a constant $C > 0$ (independent of u, x, and h) such that

$$|F_{x,X_h}(u)|^2 \leq C^2 h^{2k+1} \left\|D^{k+1} u\right\|^2_{0,X_h}, \qquad \forall u \in \mathcal{W}^{k+1,2}(X_h), \qquad \forall x \in X_h. \tag{4.7}$$

Hence,

$$\begin{aligned}
\left\|u - \mathbb{P}_{\mathcal{P}^k(X_h)} u\right\|^2_{0,X_h} &= \int_{X_h} |F_{x,X_h}(u)|^2 \, \mathrm{d}x \\
&\leq= \int_{X_h} C_2^2 h^{2k+1} \left\|D^{k+1} u\right\|^2_{0,X_h} \, \mathrm{d}x \\
&= C^2 h^{2k+2} \left\|D^{k+1} u\right\|^2_{0,X_h}, \qquad \forall u \in \mathcal{W}^{k+1,2}(X_h).
\end{aligned}$$

Taking the square root completes the proof. ∎

Corollary 4.7 (Piecewise polynomial projection)
Consider Notation 2.6. Consider a domain $X \subseteq \mathbb{R}$ and a mesh $\mathcal{X}_h = \{X_j \subseteq X\}_{j \in I \subseteq \mathbb{Z}}$ with elements with maximum diameter $h > 0$. Furthermore, let $k \geq 0$. Then,

$$\left\|u - \mathbb{P}_{\mathcal{P}^k_{\mathcal{X}_h}(X)} u\right\|_{0,X} \leq C h^{k+1} \left\|u\right\|_{q,X}, \qquad \forall u \in \mathcal{W}^{k+1,2}(X),$$

for some constant $C > 0$ (independent of h and u).

Proof:
Observe that the projection on the space of piecewise polynomials is equivalent to the elementwise projection on regular polynomial spaces:

$$\left\|u - \mathbb{P}_{\mathcal{P}^k_{\mathcal{X}_h}(X) u}\right\|^2_{0,X} = \sum_{j \in I} \left\|u|_{X_j} - \mathbb{P}_{\mathcal{P}^k(X_j)} u|_{X_j}\right\|^2_{0,X_j}, \qquad \forall u \in \mathcal{W}^{k+1,2}(X).$$

Note that the spatial domain should not be subdivided into subdomains other than the mesh elements. Apply Proposition 4.6 for each element to complete the proof. ∎

4.3 Error estimation for filtered functions in general

Now that sufficient auxiliary theory has been discussed, this section derives a (derivative) error estimation for a general class of functions to which a central spline filter has been applied.

The main result is an estimation for the $\mathcal{L}^2$-norm of the difference of (the weak derivative of) a Sobolev function and its filtered counterpart in terms of (negative-order) Sobolev norms (Theorem 4.8). The proof is based on the fact that a central spline kernel reproduces polynomials

up to a certain degree (Lemma 4.9), and the fact that derivatives of central B-splines can be expressed in terms of central difference quotients of lower order B-splines (Lemma 4.10).

In this section, the error estimation is still indepenent of the underlying physics and numerics. The next section discusses a refinement of this result for DG approximations for a one-dimensional periodic linear problem.

Theorem 4.8 (Error estimation for filtered functions in general)
Consider Notation 4.1 and a domain $X \subseteq \mathbb{R}$. Let $K^{s,s+\alpha,\{q_1,...,q_{2r-1}\}}$ be a central spline kernel (Definition 3.13), where $\alpha \in \mathbb{N}_0$ and $s, r \in \mathbb{N}_1$. Furthermore, suppose that $u_h \in \mathcal{L}^2(X)$ is an approximation to an exact solution $u \in \mathcal{W}^{2r-1+\alpha,2}(X)$. Moreover, choose $H_0 > 0$, and let $X_0 \subseteq X_1 \subseteq X$ and $X_0 \subseteq X_2 \subseteq X_3 \subseteq X_4 \subseteq X$ such that X_0 and X_1 are bounded intervals, and X_2 and X_3 are open, and, for all $H \in (0, H_0]$ and for all $m = 1, ..., 2r-1$,

$$X_0 - \operatorname{supp}\left(K_H^{s,s+\alpha,\{q_1,...,q_{2r-1}\}}\right) \subseteq X_1 \tag{4.8}$$

$$X_0 - \operatorname{supp}\left(K_H^{s+\alpha,s+\alpha,\{q_1,...,q_{2r-1}\}}\right) \subseteq X_1 \tag{4.9}$$

$$X_4 - \operatorname{supp}\left(\psi_H^s\right) - q_m + \left[-\alpha\frac{H}{2}, \alpha\frac{H}{2}\right] \subseteq X, \tag{4.10}$$

$$X_0 \Subset X_2, \tag{4.11}$$

$$X_2 - \operatorname{supp}\left(\psi_H^{s-j}\right) \subseteq X_3, \qquad \forall j = 0, ..., s-1 \tag{4.12}$$

$$X_3 + \left[-s\frac{H}{2}, s\frac{H}{2}\right] \subseteq X_4. \tag{4.13}$$

Then, there exists a constant $C > 0$ (independent of u, u_h, and H) such that

$$\left\|D^\alpha u - K_H^{s,s+\alpha,\{q_1,...,q_{2r-1}\}} \star \partial_H^\alpha u_h\right\|_{0,X_0} \leq$$
$$C\Big(H^{2r-1}\left\|u\right\|_{2r-1+\alpha,X_1} + \sum_{j=0}^{s}\left\|\partial_H^{j+\alpha}(u-u_h)\right\|_{-s,X_3}\Big), \qquad \forall H \in (0, H_0].$$

Proof:
See also [BS77, Theorem 1], [CLSS03, Theorem 3.1, Section 4.1], and [Tho77, Theorem 1]. In favour of notational brevity, the nodes $\{q_1, ..., q_{2r-1}\}$ are omitted in the notation. First, apply the triangle inequality and (4.8):

$$\left\|D^\alpha u - K_H^{s,s+\alpha} \star \partial_H^\alpha u_h\right\|_{0,X_0} \leq \left\|D^\alpha u - K_H^{s,s+\alpha} \star \partial_H^\alpha u\right\|_{0,X_0} + \left\|K_H^{s,s+\alpha} \star \partial_H^\alpha (u-u_h)\right\|_{0,X_0}$$

Because the kernel is a linear combination of central B-splines, Proposition 3.12 in combination with (4.9) implies:

$$\left(K_H^{s,s+\alpha} \star \partial_H^\alpha u\right)(x) = \frac{d^\alpha (K_H^{s+\alpha,s+\alpha} \star u)(x)}{dx^\alpha} = \left(K_H^{s+\alpha,s+\alpha} \star D^\alpha u\right)(x), \qquad \forall x \in X_0.$$

Substitution into the first term on the right hand side above gives:

$$\left\|D^\alpha u - K_H^{s,s+\alpha} \star \partial_H^\alpha u_h\right\|_{0,X_0} \leq \left\|D^\alpha u - K_H^{s+\alpha,s+\alpha} \star D^\alpha u\right\|_{0,X_0} + \left\|K_H^{s,s+\alpha} \star \partial_H^\alpha (u-u_h)\right\|_{0,X_0}.$$

The second term in the right hand side can be estimated as follows. First, write out the kernel explicitly, exploit the fact that the kernel is a linear combination of B-splines once more, and apply

a coordinate transformation:

$$\begin{aligned}\left\|K_H^{s,s+\alpha} \star \partial_H^\alpha(u-u_h)\right\|_{0,X_0} &\overset{(4.10)}{\leq} \sum_{m=1}^{2r-1} \left|\gamma_m^{s+\alpha}\right| \int_{X_0} \int_{\operatorname{supp}(\psi^s)+q_m} \psi_H^s(\xi-q_m)\partial_H^\alpha(u-u_h)(x-\xi)\,\mathrm{d}\xi\,\mathrm{d}x \\ &= \sum_{m=1}^{2r-1} \left|\gamma_m^{s+\alpha}\right| \int_{X_0} \int_{\operatorname{supp}(\psi^s)} \psi_H^s(\xi)\partial_H^\alpha(u-u_h)(x-q_m-\xi)\,\mathrm{d}\xi\,\mathrm{d}x \\ &\leq \sum_{m=1}^{2r-1} \left|\gamma_m^{s+\alpha}\right| \left\|\psi_H^s \star v^m\right\|_{0,X_0},\end{aligned}$$

where, for all $m = 1, ..., 2r-1$, the function $v^m \in \mathcal{L}^2(X_4)$ is defined such that $v^m(x) := \partial_H^\alpha(u - u_h)(x - q_m)$ for all $x \in X_4$. Next, apply Lemma 4.10, using (4.11), (4.12), and (4.13), to complete the estimation of the second term. The first term can be estimated by applying Lemma 4.9, using (4.9), to the function $D^\alpha u \in \mathcal{W}^{2r-1,2}(\mathbb{R})$, since the kernel $K^{s+\alpha,s+\alpha,\{q_1,...,q_{2r-1}\}}$ reproduces polynomials of degree $2r-2$ according to Proposition 3.18. Observing that $\|D^\alpha u\|_{2r-1,X_1} \leq \|u\|_{2r-1+\alpha,X_1}$ completes the proof. ∎

Lemma 4.9 (Estimating the first term)
Consider Notation 4.1. Let $X \subseteq \mathbb{R}$ be a domain and let $u \in \mathcal{W}^{q+1,2}(X)$. Furthermore, let $K \in \mathcal{C}_0^0(\mathbb{R})$ be a function that reproduces polynomials of degree q in the sense that

$$K \star p = p, \qquad \forall p \in \mathcal{P}^q(\mathbb{R}).$$

Additionally, for all $H > 0$, define $K_H \in \mathcal{C}_0^0(\mathbb{R})$ such that

$$K_H(x) = \frac{1}{H} K\left(\frac{x}{H}\right), \qquad \forall x \in \mathbb{R}.$$

Moreover, choose $H_0 > 0$, and let $X_0, X_1 \subseteq X$ be bounded intervals such that

$$X_0 - \operatorname{supp}(K_H) \subseteq X_1, \qquad \forall H \in (0, H_0]. \tag{4.14}$$

Then, there exists a constant $C > 0$ (independent of u and H) such that:

$$\|u - K_H \star u\|_{0,X_0} \leq C \|u\|_{q+1,X_1} H^{q+1}, \qquad \forall H \in (0, H_0].$$

Proof:
For all $x \in X_0$ and for all $H > 0$, define $X_{x,H} := x - \operatorname{supp}(K_H)$ and define linear functionals $F_{x,X_{x,H}} : \mathcal{W}^{q+1,2}(X_{x,H}) \to \mathbb{R}$ such that

$$F_{x,X_{x,H}}(v) = v(x) - \int_{\operatorname{supp}(K_H)} K_H(\xi) v(x-\xi)\,\mathrm{d}\xi, \qquad \forall x \in X_0, \qquad \forall v \in \mathcal{W}^{q+1,2}(X_{x,H}).$$

Note that $\left|F_{x,X_{x,H}}(v)\right|$ is a continuous function of x on the bounded interval X_0, since any weakly differentiable function on a bounded domain can be identified with its continuous version [Eva98, p. 269]. Next, apply Proposition 4.5 to obtain a constant $C_1 > 0$ (independent of v, x, and H) such that

$$\left|F_{x,X_{x,H}}(v)\right|^2 \leq C_1^2 \left|X_{x,H}\right|^{2q+1} \left\|D^{q+1} v\right\|_{0,X_{x,H}}^2, \qquad \forall x \in X_0, \qquad \forall v \in \mathcal{W}^{q+1,2}(X_{x,H}).$$

Hence,

$$\begin{aligned}\|u - K_H \star u\|_{0,X_0}^2 &= \int_{X_0} \left|F_{x,X_{x,H}}(u)\right|^2 \mathrm{d}x \\ &\leq C_1^2 \int_{X_0} \left|X_{x,H}\right|^{2q+1} \left\|D^{q+1} u\right\|_{0,X_{x,H}}^2 \mathrm{d}x \\ &\leq C_1^2 \left|\operatorname{supp}(K_H)\right|^{2q+1} \int_{X_0} \int_{x-\operatorname{supp}(K_H)} \left|D^{q+1} u(\xi)\right|^2 \mathrm{d}\xi\,\mathrm{d}x, \quad \forall H \in (0, H_0].\end{aligned}$$

Apply a coordinate transformation, Fubini's Theorem, and another coordinate transformation:

$$\begin{aligned}\|u - K_H \star u\|_{0,X_0}^2 &\leq C_1^2 \left|\operatorname{supp}(K_H)\right|^{2q+1} \int_{X_0} \int_{-\operatorname{supp}(K_H)} \left|D^{q+1}u(\xi' + x)\right|^2 \,\mathrm{d}\xi' \,\mathrm{d}x \\ &\leq C_1^2 \left|\operatorname{supp}(K_H)\right|^{2q+1} \int_{-\operatorname{supp}(K_H)} \int_{X_0} \left|D^{q+1}u(\xi' + x)\right|^2 \,\mathrm{d}x \,\mathrm{d}\xi' \\ &\leq C_1^2 \left|\operatorname{supp}(K_H)\right|^{2q+1} \int_{-\operatorname{supp}(K_H)} \int_{\xi'+X_0} \left|D^{q+1}u(x')\right|^2 \,\mathrm{d}x' \,\mathrm{d}\xi'\end{aligned}$$

Taking the supreme over all ξ', this becomes:

$$\begin{aligned}\|u - K_H \star u\|_{0,X_0}^2 &\leq C_1^2 \left|\operatorname{supp}(K_H)\right|^{2q+2} \sup_{\xi' \in -\operatorname{supp}(K_H)} \int_{\xi'+X_0} \left|D^{q+1}u(x')\right|^2 \,\mathrm{d}x' \\ &\leq C_1^2 \left|\operatorname{supp}(K_H)\right|^{2q+2} \int_{-\operatorname{supp}(K_H)+X_0} \left|D^{q+1}u(x')\right|^2 \,\mathrm{d}x', \qquad \forall H \in (0, H_0].\end{aligned}$$

Observing that $|\operatorname{supp}(K_H)| = |\operatorname{supp}(K)|\, H$ and using (4.14) gives:

$$\begin{aligned}\|u - K_H \star u\|_{0,X_0}^2 &\leq \underbrace{C_1^2 \left|\operatorname{supp}(K)\right|^{2q+2}}_{=:C^2} H^{2q+2} \int_{X_1} \left|D^{q+1}u(x')\right|^2 \,\mathrm{d}x' \\ &\leq C^2 \|u\|_{q+1,X_1}^2 \; H^{2q+2}, \qquad \forall H \in (0, H_0].\end{aligned}$$

Taking the square root completes the proof. ∎

Lemma 4.10 (Estimating the second term)
Consider Notation 4.1, let $X_4 \subseteq \mathbb{R}$, choose $H_0 > 0$ and domains $X_0 \subseteq X_2 \subseteq X_3 \subseteq X_4$ such that X_2 and X_3 are open, as before, and, for all $\forall H \in (0, H_0]$:

$$X_0 \Subset X_2, \tag{4.15}$$

$$X_2 - \operatorname{supp}\left(\psi_H^{s-j}\right) \subseteq X_3, \qquad \forall j = 0, ..., s-1 \tag{4.16}$$

$$X_3 + \left[-s\frac{H}{2}, s\frac{H}{2}\right] \subseteq X_4. \tag{4.17}$$

Furthermore, let $u \in \mathcal{L}^2(X_4)$ and let ψ^s be a central B-spline (Definition 3.7). Then, there exists a constant $C > 0$ (independent of u and H) such that

$$\|\psi_H^s \star u\|_{0,X_0} \leq C \sum_{j=0}^{s} \left\|\partial_H^j u\right\|_{-s,X_3}, \qquad \forall H \in (0, H_0].$$

Proof:
See also [BS77, Theorem 1] and [CLSS03, p. 591, 592]. Start by considering the case $X_4 = \mathbb{R}$. First, the claim is shown for functions $u \in \mathcal{C}_0^\infty(\mathbb{R})$. Subsequent application of Lemma 4.3 and Proposition 3.12 gives:

$$\begin{aligned}\|\psi_H^s \star u\|_{0,X_0} &\overset{(4.15)}{\leq} C \sum_{j=0}^{s} \left\|D^j \left(\psi_H^s \star u\right)\right\|_{-s,X_2} \\ &= C \sum_{j=0}^{s} \left\|\psi_H^{s-j} \star \partial_H^j u\right\|_{-s,X_2}, \qquad \forall H > 0. \end{aligned} \tag{4.18}$$

Next, use the definition of the negative-order norm, Fubini's theorem, and a coordinate transformation subsequently:

$$\begin{aligned}
&\left\|\psi_H^{s-j} \star \partial_H^j u\right\|_{-s,X_2} \\
&= \sup_{v\in\mathcal{C}_0^\infty(X_2)} \frac{\int_{X_2}\int_{\mathrm{supp}\left(\psi_H^{s-j}\right)} \psi_H^{s-j}(\xi)\partial_H^j u(x-\xi)\,\mathrm{d}\xi\, v(x)\,\mathrm{d}x}{\|v\|_{s,X_2}} \\
&= \sup_{v\in\mathcal{C}_0^\infty(X_2)} \frac{\int_{\mathrm{supp}\left(\psi_H^{s-j}\right)} \psi_H^{s-j}(\xi)\int_{X_2} \partial_H^j u(x-\xi)v(x)\,\mathrm{d}x\,\mathrm{d}\xi}{\|v\|_{s,X_2}} \\
&= \sup_{v\in\mathcal{C}_0^\infty(X_2)} \frac{\int_{\mathrm{supp}\left(\psi_H^{s-j}\right)} \psi_H^{s-j}(\xi)\int_{X_2-\xi} \partial_H^j u(x)v(x+\xi)\,\mathrm{d}x\,\mathrm{d}\xi}{\|v\|_{s,X_2}}, \qquad \forall H>0, \quad \forall j=0,...,s-1.
\end{aligned}$$

Now, take the supremum inside the integral, change the space of test functions, and use the definition of the negative order norm:

$$\begin{aligned}
&\left\|\psi_H^{s-j} \star \partial_H^j u\right\|_{-s,X_2} \\
&\le \int_{\mathrm{supp}\left(\psi_H^{s-j}\right)} \psi_H^{s-j}(\xi) \sup_{v\in\mathcal{C}_0^\infty(X_2)} \frac{\int_{X_2-\xi} \partial_H^j u(x)v(x+\xi)\,\mathrm{d}x}{\|v\|_{s,X_2}}\,\mathrm{d}\xi \\
&= \int_{\mathrm{supp}\left(\psi_H^{s-j}\right)} \psi_H^{s-j}(\xi) \sup_{v\in\mathcal{C}_0^\infty(X_2-\xi)} \frac{\int_{X_2-\xi} \partial_H^j u(x)v(x)\,\mathrm{d}x}{\|v\|_{s,X_2-\xi}}\,\mathrm{d}\xi \\
&= \int_{\mathrm{supp}\left(\psi_H^{s-j}\right)} \psi_H^{s-j}(\xi) \left\|\partial_H^j u\right\|_{-s,X_2-\xi}\,\mathrm{d}\xi, \qquad \forall H>0, \quad \forall j=0,...,s-1.
\end{aligned}$$

Estimate the negative order norm and use the fact that the integral over a B-spline is equal to 1 (cf. Proposition 3.6):

$$\begin{aligned}
\left\|\psi_H^{s-j} \star \partial_H^j u\right\|_{-s,X_2} &\overset{(4.16),(4.4)}{\le} \int_{\mathrm{supp}\left(\psi_H^{s-j}\right)} \psi_H^{s-j}(\xi) \left\|\partial_H^j u\right\|_{-s,X_3}\,\mathrm{d}\xi \\
&= \left\|\partial_H^j u\right\|_{-s,X_3}, \qquad \forall H\in(0,H_0], \quad \forall j=0,...,s-1.
\end{aligned}$$

Substitution of this result into (4.18) gives, for all $u\in\mathcal{C}_0^\infty(\mathbb{R})$:

$$\|\psi_H^s \star u\|_{0,\mathbb{R}} \le C\sum_{j=0}^{s} \left\|\partial_H^j u\right\|_{-s,X_3}, \qquad \forall H\in(0,H_0]. \tag{4.19}$$

For general functions $u\in\mathcal{L}^2(\mathbb{R})$, the claim can be shown as follows. As the space $\mathcal{C}_0^\infty(\mathbb{R})$ lies dense in $\mathcal{L}^2(\mathbb{R})$ with respect to the norm $\|.\|_{0,\mathbb{R}}$, for any $v\in\mathcal{C}_0^\infty(\mathbb{R})$, the following estimate is obtained using the triangle inequality:

$$\begin{aligned}
\|\psi_H^s \star u\|_{0,X_0} &= \|\psi_H^s \star (u-v+v)\|_{0,X_0} \\
&\le \|\psi_H^s \star (u-v)\|_{0,X_0} + \|\psi_H^s \star v\|_{0,X_0} \\
&\overset{(4.3)}{\le} \|\psi_H^s \star (u-v)\|_{0,\mathbb{R}} + \|\psi_H^s \star v\|_{0,X_0}, \qquad \forall H\in(0,H_0].
\end{aligned}$$

Applying Young's inequality for convolutions to the first term and (4.19) to the second implies:

$$\begin{aligned}
\|\psi_H^s \star u\|_{0,\mathbb{R}} &\le \underbrace{\int_{\mathbb{R}} \psi_H^s(x)\,\mathrm{d}x}_{=1} \|u-v\|_{0,\mathbb{R}} + C\sum_{j=0}^{s} \left\|\partial_H^j v\right\|_{-s,X_3} \\
&= \|u-v\|_{0,\mathbb{R}} + C\sum_{j=0}^{s} \left\|\partial_H^j\,(v-u+u)\right\|_{-s,X_3}, \qquad \forall H\in(0,H_0]
\end{aligned}$$

Applying the triangle inequality and estimating the negative-order norm yields:

$$\begin{aligned}\left\|\psi_H^s \star u\right\|_{0,\mathbb{R}} &\leq \|u-v\|_{0,\mathbb{R}} + C\sum_{j=0}^{s}\left\|\partial_H^j\,(v-u)\right\|_{-s,X_3} + C\sum_{j=0}^{s}\left\|\partial_H^j u\right\|_{-s,X_3}\\ &\overset{(4.4)}{\leq} \|u-v\|_{0,\mathbb{R}} + C\sum_{j=0}^{s}\left\|\partial_H^j\,(v-u)\right\|_{-s,\mathbb{R}} + C\sum_{j=0}^{s}\left\|\partial_H^j u\right\|_{-s,X_3}, \quad \forall H\in(0,H_0].\end{aligned}$$

The divided difference can be rewritten as follows:

$$\begin{aligned}\left\|\partial_H u'\right\|_{-s,\mathbb{R}} &= \sup_{w\mathcal{C}_0^\infty(\mathbb{R})} \frac{\int_{\mathbb{R}}\left(u'(x+\frac{H}{2}) - u'(x-\frac{H}{2})\right)w(x)\,\mathrm{d}x}{H\left\|w\right\|_{s,\mathbb{R}}}\\ &\leq \sup_{w\mathcal{C}_0^\infty(\mathbb{R})} \frac{2\int_{\mathbb{R}} u'(x)w(x)\,\mathrm{d}x}{H\left\|w\right\|_{s,\mathbb{R}}}\\ &= \frac{2}{H}\left\|u'\right\|_{-s,\mathbb{R}}, \qquad \forall H>0, \quad \forall u'\in\mathcal{L}^2(\mathbb{R}). \quad (4.20)\end{aligned}$$

This implies:

$$\left\|\psi_H^s \star u\right\|_{0,\mathbb{R}} \leq \|u-v\|_{0,\mathbb{R}} + C\sum_{j=0}^{s}\left(\frac{2}{H}\right)^j\|v-u\|_{-s,\mathbb{R}} + C\sum_{j=0}^{s}\left\|\partial_H^j u\right\|_{-s,X_3}, \quad \forall H\in(0,H_0].$$

Apply (4.2) to estimate the negative-order norms in terms of $\mathcal{L}^2$-norms:

$$\left\|\psi_H^s \star u\right\|_{0,\mathbb{R}} \leq \|u-v\|_{0,\mathbb{R}} + C\sum_{j=0}^{s}\left(\frac{2}{H}\right)^j\|v-u\|_{0,\mathbb{R}} + C\sum_{j=0}^{s}\left\|\partial_H^j u\right\|_{-s,X_3}, \quad \forall H\in(0,H_0].$$

The first two terms become arbitrarily small, as the space $\mathcal{C}_0^\infty(\mathbb{R})$ lies dense in $\mathcal{L}^2(\mathbb{R})$ with respect to the norm $\|.\|_{0,\mathbb{R}}$, which completes the proof for $X_4=\mathbb{R}$. Next, consider general $X_4\subseteq\mathbb{R}$ and let $u\in\mathcal{L}^2(X_4)$. Define $v\in\mathcal{L}^2(\mathbb{R})$ such that $v|_{X_4}=u$. Applying the result for functions in $\mathcal{L}^2(\mathbb{R})$ gives:

$$\begin{aligned}\left\|\psi_H^s \star u\right\|_{0,X_0} &\overset{(4.16)}{=} \int_{X_0}\int_{\mathrm{supp}\left(\psi_H^s\right)}\psi_H^s(\xi)u(x-\xi)\,\mathrm{d}\xi\,\mathrm{d}x = \left\|\psi_H^s\star v\right\|_{0,X_0}\\ &\leq C\sum_{j=0}^{s}\left\|\partial_H^j v\right\|_{-s,X_3} \overset{(4.17)}{=} C\sum_{j=0}^{s}\left\|\partial_H^j u\right\|_{-s,X_3}, \qquad \forall H\in(0,H_0],\end{aligned}$$

which completes the proof. ∎

4.4 Error estimation for filtered DG approximations

The previous section derived a (derivative) error estimation for a general class of functions to which a central spline filter has been applied. This section uses the characteristics of the DG method to refine this error estimation for DG approximations.

The main challenge of this section is to find an estimate for the negative-order norm of the central difference quotient of the difference between the filtered and the unfiltered function (cf. Theorem 4.8). To obtain this result, first, an auxiliary estimation is derived using the linearity and the periodicity of the hyperbolic problem under consideration (Lemma 4.12). This estimation contains the sum of three terms, which are estimated by three lemmas (Lemma 4.13, Lemma 4.14, and Lemma 4.15). These lemmas make use of the characteristics of the DG scheme and the fact that the $\mathcal{L}^2$-projection of a function on a polynomial space is close to its unprojected counterpart. After that, the required estimation for the negative-order norm of the central difference quotient

is obtained (Theorem 4.16). By combining this result with Theorem 4.8, the final (derivative) error estimation for DG approximations is obtained (Theorem 4.17). This result holds for DG approximations based on the first-order upwind flux and exact time integration on one-dimensional non-equidistant meshes for periodic linear hyperbolic equations with a sufficiently smooth exact solution.

From this error estimation four conclusions can be drawn. One: for any B-spline order, i.e. for any required order of differentiability of the filtered DG approximation, there exists a number of nodes for which the corresponding central spline filter at least conserves the convergence rate of the DG approximation, i.e. $k+1$. Two: as the number of nodes tends to infinity, the convergence rate of the filtered DG approximation approaches $2k+1$, which is the same order as for equidistant meshes with $2k+1$ nodes [CJST98, p. 585]. Three: for larger numbers of k, fewer nodes are required then are traditionally being used (Remark 4.18). Four: these three conclusions also apply for the extraction of an approximation of the derivatives of the exact solution from its DG approximation through central spline filtering. The question is whether it is possible to use such derivative information in an ODE solver that is particularly suitable for streamline visualisation.

Notation 4.11 (Linear hyperbolic problem)
Consider Notation 2.6, Notation 4.1 and Example 2.8 for $u \in \mathcal{C}^1\big(T, \mathcal{W}^{k+1,2}(X)\big)$ and rewrite the DG scheme (2.7) as follows:

$$\left\langle \frac{\partial u_h}{\partial t}(t), v \right\rangle_X + B\big(u_h(t), v\big) = 0, \qquad \forall v \in \mathcal{P}^k_{\mathcal{X}_h}(X), \tag{4.21}$$

where $B : \mathcal{C}^1_{\mathcal{X}_h}(X) \times \mathcal{C}^1_{\mathcal{X}_h}(X) \to X$ is the following bilinear form:

$$\begin{aligned} B\big(w, v\big) &= \sum_{j \in I} \left(\left\langle -cw^j, \frac{\partial v^j}{\partial x} \right\rangle_{X_j} + \left[cw^j\, v^j \right]_{x_{j+\frac{1}{2}}} + \left[-cw^{j'-1}\, v^j \right]_{x_{j-\frac{1}{2}}} \right) && (4.22) \\ &= \sum_{j \in I} \left(\left\langle w^j, -c\frac{\partial v^j}{\partial x} \right\rangle_{X_j} + \left[cw^j\, v^j \right]_{x_{j+\frac{1}{2}}} + \left[-cw^{j'-1}\, v^j \right]_{x_{j-\frac{1}{2}}} \right) && (4.23) \\ &= \sum_{j \in I} \left(\left\langle c\frac{\partial w^j}{\partial x}, v^j \right\rangle_{X_j} + \left[c(w^j - w^{j'-1})\, v^j \right]_{x_{j-\frac{1}{2}}} \right). && (4.24) \end{aligned}$$

The third equation can de derived using integration by parts. Moreover, for all $w \in \mathcal{C}^\infty_0(\mathrm{int}(X))$, let $v_w \in \mathcal{C}^1\big(T, \mathcal{C}^\infty(X)\big)$ satisfy periodic boundary conditions and:

$$\begin{aligned} \frac{\partial v_w}{\partial t}(t) + c\frac{\partial v_w(t)}{\partial x} &= 0, \qquad \forall t \in T, && (4.25) \\ v_w(t_b) &= w, && (4.26) \end{aligned}$$

which is also referred to as the dual problem. ⌟

Lemma 4.12 (Auxiliary estimate with three terms)
Consider Notation 4.11. Then,

$$\begin{aligned} \langle u(t_b) - u_h(t_b), w \rangle_X = \langle u(t_a) - u_h(t_a), v_w(t_a) \rangle_X \\ - \int_{t_a}^{t_b} \left(\left\langle \frac{\partial u_h}{\partial t}(t), v_w(t) - v(t) \right\rangle_X + B\big(u_h(t), v_w(t) - v(t)\big) \right) \mathrm{d}t \\ - \int_{t_a}^{t_b} \left(\left\langle u_h(t), \frac{\partial v_w}{\partial t}(t) \right\rangle_X - B\big(u_h(t), v_w(t)\big) \right) \mathrm{d}t, \end{aligned}$$

for all $v : T \to \mathcal{P}^k_{\mathcal{X}_h}(X)$ and for all $w \in \mathcal{C}^\infty_0(\mathrm{int}(X))$.

PROOF:
See also [CLSS03, p. 588]. First, apply (4.26):

$$\langle u(t_b) - u_h(t_b), w\rangle_X = \langle u(t_b), v_w(t_b)\rangle_X - \langle u_h(t_b), v_w(t_b)\rangle_X$$

Apply (2.5) together with (4.25) and the periodic boundary conditions to the first term, and the Fundamental Theorem of Calculus to the second:

$$\begin{aligned}\langle u(t_b) - u_h(t_b), w\rangle_X &= \langle u(t_a), v_w(t_a)\rangle_X - \langle u_h(t_a), v_w(t_a)\rangle_X - \int_{t_a}^{t_b} \frac{\partial \langle u_h, v_w\rangle_X}{\partial t}(t)\,\mathrm{d}t \\ &= \langle u(t_a) - u_h(t_a), v_w(t_a)\rangle_X - \int_{t_a}^{t_b} \frac{\partial \langle u_h, v_w\rangle_X}{\partial t}(t)\,\mathrm{d}t. \\ &= \langle u(t_a) - u_h(t_a), v_w(t_a)\rangle_X \\ &\quad - \int_{t_a}^{t_b} \left(\left\langle \frac{\partial u_h}{\partial t}(t), v_w(t)\right\rangle_X + \left\langle u_h(t), \frac{\partial v_w}{\partial t}(t)\right\rangle_X \right) \mathrm{d}t.\end{aligned}$$

Use (4.21) to obtain, for all $v : T \to \mathcal{P}^k_{\mathcal{X}_h}(X)$:

$$\begin{aligned}\int_{t_a}^{t_b} \left\langle \frac{\partial u_h}{\partial t}(t), v_w(t)\right\rangle_X \mathrm{d}t &= \int_{t_a}^{t_b} \left\langle \frac{\partial u_h}{\partial t}(t), v_w(t) - v(t)\right\rangle_X \mathrm{d}t + \int_{t_a}^{t_b} \left\langle \frac{\partial u_h}{\partial t}(t), v(t)\right\rangle_X \mathrm{d}t \\ &\overset{(4.21)}{=} \int_{t_a}^{t_b} \left\langle \frac{\partial u_h}{\partial t}(t), v_w(t) - v(t)\right\rangle_X \mathrm{d}t - \int_{t_a}^{t_b} B\big(u_h(t), v(t)\big)\,\mathrm{d}t \\ &= \int_{t_a}^{t_b} \left\langle \frac{\partial u_h}{\partial t}(t), v_w(t) - v(t)\right\rangle_X \mathrm{d}t + \int_{t_a}^{t_b} B\big(u_h(t), v_w(t) - v(t)\big)\,\mathrm{d}t \\ &\quad - \int_{t_a}^{t_b} B\big(u_h(t), v_w(t)\big)\,\mathrm{d}t.\end{aligned}$$

Substitution of this result completes the proof. ∎

Lemma 4.13 (Estimating the first term: projection)
Consider Notation 4.11. Then, there exists a constant $C > 0$ (independent of u, u_h, w, and h) such that:

$$|\langle u(t_a) - u_h(t_a), v_w(t_a)\rangle_X| \leq C\,\|u(t_a)\|_{k+1,X}\,\|w\|_{k+1,X}\,h^{2k+2}, \quad \forall h > 0, \quad \forall w \in \mathcal{C}_0^\infty(\mathrm{int}(X)).$$

PROOF:
See also [CLSS03, p. 589, 592, 593]. Because $u_h(t_a) = \mathbb{P}_{\mathcal{P}^k_{\mathcal{X}_h}(X)}\big(u(t_a)\big)$,

$$\left\langle u(t_a) - u_h(t_a), \mathbb{P}_{\mathcal{P}^k_{\mathcal{X}_h}(X)}\big(v_w(t_a)\big)\right\rangle_X = 0.$$

Use this result together with the Cauchy-Schwartz inequality:

$$\begin{aligned}|\langle u(t_a) - u_h(t_a), v_w(t_a)\rangle_X| &= \left|\left\langle u(t_a) - u_h(t_a), v_w(t_a) - \mathbb{P}_{\mathcal{P}^k_{\mathcal{X}_h}(X)}\big(v_w(t_a)\big)\right\rangle_X\right| \\ &\leq \|u(t_a) - u_h(t_a)\|_{0,X} \left\|v_w(t_a) - \mathbb{P}_{\mathcal{P}^k_{\mathcal{X}_h}(X)}\big(v_w(t_a)\big)\right\|_{0,X}. \qquad (4.27)\end{aligned}$$

Because $u_h(t_a) = \mathbb{P}_{\mathcal{P}^k_{\mathcal{X}_h}(X)}\big(u(t_a)\big)$, it follows from Corollary 4.7 that there exists a constant $C_1 > 0$ such that

$$\|u(t_a) - u_h(t_a)\|_{0,X} \leq C_1 h^{k+1}\,\|u(t_a)\|_{k+1,X}\,.$$

Similarly, there exists a constant C_2 such that

$$\left\|v_w(t_a) - \mathbb{P}_{\mathcal{P}^k_{\mathcal{X}_h}(X)}\big(v_w(t_a)\big)\right\|_{0,X} \leq C_2 h^{k+1}\,\|v_w(t_a)\|_{k+1,X}\,.$$

As $v_w(t_a)$ is a periodic translation of $v_w(t_b)$, their Sobolev norms are equal:

$$\|v_w(t_a)\|_{k+1,X} = \|v_w(t_b)\|_{k+1,X} \overset{(4.26)}{=} \|w\|_{k+1,X}\,.$$

Substitution of these results into (4.27) ends the proof. ∎

Lemma 4.14 (Estimating the second term: residual)
Consider Notation 4.11, and suppose that $u \in \mathcal{W}^{k+1,2}(X)$. Then, there exists a constant $C > 0$ (independent of u, u_h, w, and h) and a function $v : T \to \mathcal{P}^k_{\mathcal{X}_h}(X)$ such that:

$$\left|\int_{t_a}^{t_b}\left(\left\langle\frac{\partial u_h}{\partial t}(t), v_w(t)-v(t)\right\rangle_X + B\big(u_h(t), v_w(t)-v(t)\big)\right)\mathrm{d}t\right| \le C\,\|u(t_a)\|_{k+1,X}\,\|w\|_{k+1,X}\,h^{2k+1},$$
$$\forall h>0, \qquad \forall w \in \mathcal{C}_0^\infty(\mathrm{int}(X)).$$

Proof:
See also [CLSS03, p. 589, 592, 593]. Note that:

$$\begin{aligned}\left\langle\frac{\partial u_h}{\partial t}(t), v_w(t)-v(t)\right\rangle_X + B\big(u_h(t), v_w(t)-v(t)\big) \overset{(4.24)}{=}\\ \sum_{j\in I}\left(\left\langle\frac{\partial u_h^j}{\partial t}(t) + c\frac{\partial u_h^j(t)}{\partial x}, v_w^j(t)-v^j(t)\right\rangle_{X_j}\right.\\ \left.+\left[c\big(u_h^j(t)-u_h^{j'-1}(t)\big)\big(v_w^j(t)-v^j(t)\big)\right]_{x_{j-\frac12}}\right)\end{aligned}$$

Next, choose $v(t) := \mathbb{P}_{\mathcal{P}^k_{\mathcal{X}_h}} v_w(t)$, for all $t \in T$. Because $u_h(t) \in \mathcal{P}^k_{\mathcal{X}_h}(X)$ for all $t \in T$, the inner product above is then equal to zero:

$$\begin{aligned}&\left\langle\frac{\partial u_h}{\partial t}(t), v_w(t)-v(t)\right\rangle_X + B\big(u_h(t), v_w(t)-v(t)\big)\\ =&\sum_{j\in I}\left[c\big(u_h^j(t)-u_h^{j'-1}(t)\big)\big(v_w^j(t)-v^j(t)\big)\right]_{x_{j-\frac12}}.\end{aligned}$$

Integrate over time and apply the Cauchy-Schwarz inequality:

$$\begin{aligned}&\left|\int_{t_a}^{t_b}\left(\left\langle\frac{\partial u_h}{\partial t}(t), v_w(t)-v(t)\right\rangle_X + B\big(u_h(t), v_w(t)-v(t)\big)\right)\mathrm{d}t\right| \le\\ &\left(\int_{t_a}^{t_b}\sum_{j\in I}\left[c\big(u_h^j(t)-u_h^{j'-1}(t)\big)\right]^2_{x_{j-\frac12}}\mathrm{d}t\right)^{\frac12}\left(\int_{t_a}^{t_b}\sum_{j\in I}\left[v_w^j(t)-v^j(t)\right]^2_{x_{j-\frac12}}\right)^{\frac12}.\end{aligned} \tag{4.28}$$

The second term can be estimated as follows. First, apply (4.7) to obtain a constant $C_0 > 0$ (independent of v_w, and h) such that

$$\left|\left[v_w^j(t)-v^j(t)\right]_{x_{j-\frac12}}\right| \le C_0 h^{k+\frac12}\,\|v_w\|_{k+1,X_j}$$

Take the square and sum over all of the elements:

$$\sum_{j\in I}\left[v_w^j(t)-v^j(t)\right]^2_{x_{j-\frac12}} \le C_0^2 h^{2k+1}\,\|v_w\|^2_{k+1,X}\,.$$

To estimate the first term in (4.28), proceed as follows. First, use the triangle inequality:

$$
\begin{aligned}
&\left| c\left[u_h^j(t) - u_h^{j'-1}(t)\right]_{x_{j-\frac{1}{2}}} \right| \\
=&\Big| c\Big[u_h^j(t) - \mathbb{P}_{\mathcal{P}^k_{\mathcal{X}_h}} u^j(t) + \mathbb{P}_{\mathcal{P}^k_{\mathcal{X}_h}} u^j(t) - u^j(t) + u^j(t) - u^{j'-1}(t) \\
&\quad + u^{j'-1}(t) - \mathbb{P}_{\mathcal{P}^k_{\mathcal{X}_h}} u^{j'-1}(t) + \mathbb{P}_{\mathcal{P}^k_{\mathcal{X}_h}} u^{j'-1}(t) - u_h^{j'-1}(t)\Big]_{x_{j-\frac{1}{2}}} \Big| \\
\leq&\left| c\left[u_h^j(t) - \mathbb{P}_{\mathcal{P}^k_{\mathcal{X}_h}} u^j(t)\right]_{x_{j-\frac{1}{2}}} + c\left[\mathbb{P}_{\mathcal{P}^k_{\mathcal{X}_h}} u^{j'-1}(t) - u_h^{j'-1}(t)\right]_{x_{j-\frac{1}{2}}} \right| \\
&+ \left| c\left[\mathbb{P}_{\mathcal{P}^k_{\mathcal{X}_h}} u^j(t) - u^j(t)\right]_{x_{j-\frac{1}{2}}} \right| + \left| c\left[u^{j'-1}(t) - \mathbb{P}_{\mathcal{P}^k_{\mathcal{X}_h}} u^{j'-1}(t)\right]_{x_{j-\frac{1}{2}}} \right| \\
&+ \left| c\left[u^j(t) - u^{j'-1}(t)\right]_{x_{j-\frac{1}{2}}} \right|, \qquad \forall j \in I.
\end{aligned}
$$

The second and third terms can be estimated with the help of Proposition 4.5. The last term vanishes, because the exact solution is continuous.:

$$
\begin{aligned}
&\left| c\left[u_h^j(t) - u_h^{j'-1}(t)\right]_{x_{j-\frac{1}{2}}} \right| \\
\leq&\left| c\left[u_h^j(t) - \mathbb{P}_{\mathcal{P}^k_{\mathcal{X}_h}} u^j(t)\right]_{x_{j-\frac{1}{2}}} - c\left[u_h^{j'-1}(t) - \mathbb{P}_{\mathcal{P}^k_{\mathcal{X}_h}} u^{j'-1}(t)\right]_{x_{j-\frac{1}{2}}} \right| \\
&+ C_1 h^{k+\frac{1}{2}} \|u\|_{k+1,X_j} + C_1 h^{k+\frac{1}{2}} \|u\|_{k+1,X_{j'-1}}, \qquad \forall j \in I.
\end{aligned}
$$

for some constant $C_1 > 0$ (independent of u, and h. Take the square, sum over the elements, and use the equivalence of the ℓ^1-norm and ℓ^2-norm for finite dimensions:

$$
\begin{aligned}
&\sum_{j\in I} c\left[u_h^j(t) - u_h^{j'-1}(t)\right]^2_{x_{j-\frac{1}{2}}} \\
\leq& C_2 \sum_{j\in I} \left| c\left[u_h^j(t) - \mathbb{P}_{\mathcal{P}^k_{\mathcal{X}_h}} u^j(t)\right]_{x_{j-\frac{1}{2}}} + c\left[\mathbb{P}_{\mathcal{P}^k_{\mathcal{X}_h}} u^{j'-1}(t) - u_h^{j'-1}(t)\right]_{x_{j-\frac{1}{2}}} \right|^2 \\
&+ 2C_1 C_2 h^{2k+1} \|u\|^2_{k+1,X},
\end{aligned}
$$

for some constant $C_2 > 0$ (independent of u, and h). Making use of [CJST98, inequality at the bottom of p. 196] yields the estimate for the first term:

$$
\sum_{j\in I} c\left[u_h^j(t) - u_h^{j'-1}(t)\right]^2_{x_{j-\frac{1}{2}}} \leq C_2 C_3 h^{2k+1} \|u\|^2_{k+1,X} + 2C_1 C_2 h^{2k+1} \|u\|^2_{k+1,X},
$$

for some constant $C_3 > 0$ (independent of u, and h. Substitution of these two estimates into (4.28) completes the proof. ∎

Lemma 4.15 (Estimating the third term: consistency)
Consider Notation 4.11. Then,

$$
\left| \int_{t_a}^{t_b} \left(\left\langle u_h(t), \frac{\partial v_w}{\partial t}(t) \right\rangle_X - B\big(u_h(t), v_w(t)\big) \right) \mathrm{d}t \right| = 0, \qquad \forall h > 0, \qquad \forall w \in \mathcal{C}_0^\infty(\mathrm{int}(X)).
$$

PROOF:
See also [CLSS03, p. 589, 592, 593]. First, rewrite the integrand:

$$\begin{aligned}
&\left\langle u_h(t), \frac{\partial v_w}{\partial t}(t) \right\rangle_X - B\big(u_h(t), v_w(t)\big) \overset{(4.25)}{=} \\
&\left\langle u_h(t), -c_1 \frac{\partial v_w(t)}{\partial x} \right\rangle_X - B\big(u_h(t), v_w(t)\big) \overset{(4.23)}{=} \\
&-\sum_{j\in I} \left(\Big[c_1 u_h^j(t) v_w^j(t)\Big]_{x_{j+\frac{1}{2}}} + \Big[-c_1 u_h^{j'-1}(t) v_w^j(t)\Big]_{x_{j-\frac{1}{2}}} \right), \qquad \forall t \in [t_a, t_b].
\end{aligned}$$

Because of the periodic boundary conditions and the fact that $v_w(t)$ is continuous (for all $t \in [t_a, t_b]$), the integrand is zero:

$$\begin{aligned}
&\left\langle u_h(t), \frac{\partial v_w}{\partial t}(t) \right\rangle_X - B\big(u_h(t), v_w(t)\big) = \\
&-\sum_{j\in I} \Big[c_1 u_h^j(t) v_w^j(t)\Big]_{x_{j+\frac{1}{2}}} + \sum_{j\in I} \Big[c_1 u_h^j(t) v_w^j(t)\Big]_{x_{j+\frac{1}{2}}} = 0, \qquad \forall t \in [t_a, t_b].
\end{aligned}$$

As the integrand is equal to zero, so is the integral. ∎

Theorem 4.16 (Estimating the negative-order norm of the divided difference)
Consider Notation 4.11, let $j \in \mathbb{N}_0$ and let $s \geq k+1$. Furthermore, choose $H_0 > 0$ and open $X_3 \subseteq X$ such that

$$X_3 + \left[-j\frac{H}{2}, j\frac{H}{2}\right] \subseteq \operatorname{int}(X), \qquad \forall H \in (0, H_0] \tag{4.29}$$

Then, there exists a constant $C > 0$ (independent of u, u_h and h) such that:

$$\left\| \partial_H^j \big(u(t_b) - u_h(t_b)\big) \right\|_{-s, X_3} \leq C \left\| u(t_a) \right\|_{k+1,X} h^{2k+1} H^{-j}, \quad \forall H \in (0, H_0], \quad \forall h > 0. \tag{4.30}$$

PROOF:
See also [Tho77, p. 589, 590]. By applying Lemma 4.12, Lemma 4.13, Lemma 4.14, and Lemma 4.15 for $w \in \mathcal{C}_0^\infty(\operatorname{int}(X))$ it follows that there exists a constant $C > 0$ (independent of u and u_h) such that:

$$\begin{aligned}
\left\| u(t_b) - u_h(t_b) \right\|_{-s, X_3} &\overset{(4.2),(4.4)}{\leq} \left\| u(t_b) - u_h(t_b) \right\|_{-(k+1), \operatorname{int}(X)} \\
&\leq C \left\| u(t_a) \right\|_{k+1,X} h^{2k+1}, \qquad \forall H \in (0, H_0), \quad \forall h > 0.
\end{aligned}$$

This completes the proof for $j = 0$. For general $j \in \mathbb{N}_0$, proceed as follows:

$$\begin{aligned}
&\left\| \partial_H^j \big(u(t_b) - u_h(t_b)\big) \right\|_{-s, X_3} \\
&\overset{\text{cf. } (4.20),(4.29)}{\leq} \left(\frac{2}{H}\right)^j \left\| u(t_b) - u_h(t_b) \right\|_{-s, \operatorname{int}(X)}, \qquad \forall H \in (0, H_0], \qquad \forall h > 0.
\end{aligned}$$

Due to the result for $j = 0$ above, there exists a constant $C_1 > 0$ (independent of u and u_h) such that:

$$\left\| \partial_H^j \big(u(t_b) - u_h(t_b)\big) \right\|_{-s, X_3} \leq \underbrace{C_1 2^j}_{=:C} \left\| u(t_a) \right\|_{k+1,X} h^{2k+1} H^{-j}, \quad \forall H \in (0, H_0], \quad \forall h > 0,$$

which completes the proof. ∎

Theorem 4.17 (Conservation of convergence rate)
Consider Notation 4.1 and Notation 4.11 and the notation of Theorem 4.8. Additionally, assume that $s \geq k+1$ and that $u \in \mathcal{W}^{\max\{k+1,2r-1+\alpha\},2}(X)$. Then, there exists a constant $C > 0$ (independent of u, u_h, H, and h) such that:

$$\left\| D^\alpha u - K_H^{s,s+\alpha,\{q_1,\ldots,q_{2r-1}\}} \star \partial_H^\alpha u_h \right\|_{0,X_0} \leq$$
$$C \max\left\{ \|u(t_b)\|_{2r-1+\alpha,X}, \|u(t_a)\|_{k+1,X} \right\} h^{\frac{2k+1}{2r-1+s+\alpha}(2r-1)}, \qquad \forall H := h^{\frac{2k+1}{2r-1+s+\alpha}} \in (0, H_0].$$

In particular, for

$$r \geq \frac{(k+1)(s+\alpha)+k}{2k},$$

the convergence rate of the filtered DG approximation is at least $k+1$, which implies conservation of convergence. Furthermore, for $r \to \infty$, the convergence rate approaches $2k+1$.

Proof:
See also [CLSS03, Corollary 3.2, Theorem 3.4]. It follows from Theorem 4.8 and Theorem 4.16 that there exists a constant $C > 0$ such that

$$\left\| D^\alpha u - K_H^{s,s+\alpha,\{q_1,\ldots,q_{2r-1}\}} \star \partial_H^\alpha u_h \right\|_{0,X_0} \leq$$
$$C \left(\|u(t_b)\|_{2r-1+\alpha,X_1} H^{2r-1} + \|u(t_a)\|_{k+1,X} h^{2k+1} H^{-s-\alpha} \right), \qquad \forall h > 0, \quad \forall H \in (0, H_0].$$

Application of (4.3) to the first term on he right hand side and substitution of $H := h^{\frac{2k+1}{2r-1+s+\alpha}}$ completes the proof. ∎

Remark 4.18 (Requiring fewer nodes)
Presently, often the choice $s = r = k+1$ is made (cf. [RS03, Section 2], [RSA05, Section 1.2]). This choice originates from the error estimations for equidistant meshes, which imply convergence of order $2r+1$ [CJST98, p. 585], However, if merely conservation of the convergence rate is sought, for larger numbers of k, fewer nodes than $2r+1$ are required. For example, if $k = 4$ and if the B-spline order equals $k+1 = 5$, then $r = k$ is sufficient, which corresponds to $2k-1$ nodes. This can help to reduce computational costs. ⌟

4.5 Conclusion

This chapter has derived a derivative error estimation for central spline filtered DG approximations based on the first-order upwind flux and exact time integration on one-dimensional non-equidistant meshes for periodic linear hyperbolic equations with a sufficiently smooth exact solution. Among other things, it can be concluded from this error estimation that, for any B-spline order, i.e. for any required order of differentiability of the filtered DG approximation, there exists a number of nodes for which the corresponding central spline filter at least conserves the convergence rate of the DG approximation, i.e. $k+1$.

Chapter 5

Conclusion

The Discontinuous Galerkin (DG) method is a flexible method for approximating the solution of a hyperbolic system. Its flexibility is mainly due to the fact that its outcome is allowed to be discontinuous at the element boundaries. This can in turn become a disadvantage, because a lack of smoothness can have a negative effect on the accuracy of the visualisation of the DG approximation, e.g. in the form of streamlines. The main goal of this research is to tackle this problem through spline filtering.

A central spline filter convolves the function to be filtered against a central spline kernel, which is a linear combination of central B-splines. The filter enhances the smoothness in the sense that the filtered solution is at least differentiable up to the order of the central B-splines minus two. This can benefit the accuracy of streamline visualisation. Additionally, a reduction of oscillations in the error is observed. At the same time, it can be shown that a central spline filter at least conserves the convergence rate for a certain class of problems.

Based on this literature study, the following research questions arise:

- Defining the problem:
  - What order of differentiability is required precisely for proper streamline visualisation? Are there ODE solvers that are capable of dealing with discontinuities? What are their disadvantages?
- Increasing the smoothness:
  - Most likely, the use of different kernels throughout the domain is inevitable in order enhance the practical applicability discussed below. Unfortunately, a non-smooth variation in the kernels can introduce non-smoothness in the filtered solution (cf. [RS03]). Is it possible to construct smooth transitions to circumvent this issue?
- Conserving the convergence:
  - The current theoretical error estimations for spline filtered DG approximations do not apply for
    - non-linear problems,
    - problems with non-periodic boundary conditions,
    - problems with an insufficiently smooth exact solution (e.g. shocks),
    - inexact time integration,
    - a numerical flux function other than the first-order upwind flux function,
    - a certain region that is adjacent to the boundary of the spatial domain and that typically spans multiple elements,
    - triangular meshes in the multi-dimensional case.

In other words, the current error estimations do not apply for most real-life applications. Is it possible to improve on the existing spline filters to increase their practical applicability for some of the classes above?

- With respect to one-dimensional filtering along the streamline in a two-dimensional domain, two questions arise:
  - Do the error estimations for one-dimensional spline filters remain valid if they are applied along a curve in a two-dimensional domain?
  - The computation of the next point on a streamline, using the one-dimensional approach with the one-sided filter, requires a continuous 'previous solution' instead of a discrete one. Previously, this problem was dealt with by using piecewise linear approximations of the streamline. How large is the error resulting from this approximation? What alternatives provide more accurate results?

- Other questions:
  - Can derivative spline filtering be used to devise an (implicit) ODE scheme that is particularly useful for streamline visualisation?
  - Unlike the symmetric filter, the one-sided filter can be applied near boundaries. Unfortunately, at the boundary, the one-sided filter is inconsistent with the boundary condition in the sense that the filtered boundary is not equal to the boundary condition. What type of filtering can deal with this problem? Could the solution to this problem make use of a kernel that looks more like a Dirac distribution as it is applied closer to the boundary?

The main focus of this research will be on the construction of a spline filter that is consistent with the boundary conditions and that can handle triangular meshes that may contain abrubt changes in mesh size.

Acknowledgments

This research is sponsored by the Air Force Office of Scientific Research, Air Force Material Command, USAF, under grant number FA8655-09-1-3055. The U.S. Government is authorized to reproduce and distribute reprints for Governmental purposes notwithstanding any copyright notation thereon.

Bibliography

[BH70] J. H. Bramble and S. R. Hilbert. Estimation of linear functionals on Sobolev spaces with application to Fourier transforms and spline interpolation. *SIAM J. Numer. Anal.*, 7:112–124, 1970.

[BH71] J. H. Bramble and S. R. Hilbert. Bounds for a class of linear functionals with applications to Hermite interpolation. *Numer. Math.*, 16:362–369, 1971.

[BS76] J. H. Bramble and A. H. Schatz. Estimates for spline projections. *Rev. Française Automat. Informat. Recherche Opérationnelle*, 10(R-2):5–37, 1976.

[BS77] J. H. Bramble and A. H. Schatz. Higher order local accuracy by averaging in the finite element method. *Math. Comp.*, 31(137):94–111, 1977.

[CJST98] B. Cockburn, C. Johnson, C.W. Shu, and E. Tadmor. *Advanced numerical approximation of nonlinear hyperbolic equations*, volume 1697 of *Lecture Notes in Mathematics*. Springer-Verlag, Berlin, 1998. Papers from the C.I.M.E. Summer School held in Cetraro, June 23–28, 1997, Edited by Alfio Quarteroni, Fondazione C.I.M.E.. [C.I.M.E. Foundation].

[CLSS03] Bernardo Cockburn, Mitchell Luskin, Chi-Wang Shu, and Endre Süli. Enhanced accuracy by post-processing for finite element methods for hyperbolic equations. *Math. Comp.*, 72(242):577–606 (electronic), 2003.

[Con85] John B. Conway. *A course in functional analysis*, volume 96 of *Graduate Texts in Mathematics*. Springer-Verlag, New York, 1985.

[CS66] H.B. Curry and I.J. Schoenberg. On Pólya frequency functions. IV. The fundamental spline functions and their limits. *J. Analyse Math.*, 17:71–107, 1966.

[Dav75] Philip J. Davis. *Interpolation and approximation*. Dover Publications Inc., New York, 1975. Republication, with minor corrections, of the 1963 original, with a new preface and bibliography.

[Eva98] Lawrence C. Evans. *Partial differential equations*, volume 19 of *Graduate Studies in Mathematics*. American Mathematical Society, Providence, RI, 1998.

[LKJ+05] D.H. Laidlaw, R.M. Kirby, J.S. Jackson, C.D. Davidson, T.S. Miller, M. da Silva, W.H. Warren, and M.J. Tarr. Comparing 2d vector field visualization methods: A user study. *IEEE Transactions on Visualization and Computer Graphics*, 11:59–70, 2005.

[Nür89] Günther Nürnberger. *Approximation by spline functions*. Springer-Verlag, Berlin, 1989.

[RS03] Jennifer Ryan and Chi-Wang Shu. On a one-sided post-processing technique for the discontinuous Galerkin methods. *Methods Appl. Anal.*, 10(2):295–307, 2003.

[RSA05] Jennifer Ryan, Chi-Wang Shu, and Harold Atkins. Extension of a postprocessing technique for the discontinuous Galerkin method for hyperbolic equations with application to an aeroacoustic problem. *SIAM J. Sci. Comput.*, 26(3):821–843 (electronic), 2005.

[Sch73] I. J. Schoenberg. *Cardinal spline interpolation*. Society for Industrial and Applied Mathematics, Philadelphia, Pa., 1973. Conference Board of the Mathematical Sciences Regional Conference Series in Applied Mathematics, No. 12.

[Sch81] Larry L. Schumaker. *Spline functions: basic theory*. John Wiley & Sons Inc., New York, 1981. Pure and Applied Mathematics, A Wiley-Interscience Publication.

[SCKR08] M. Steffen, S. Curtis, R.M. Kirby, and J.K. Ryan. Investigation of smoothness-increasing accuracy-conserving filters for improving streamline integration through discontinuous fields. *IEEE Transactions on Visualization and Computer Graphics*, 14:680–692, 2008.

[Tho77] Vidar Thomée. High order local approximations to derivatives in the finite element method. *Math. Comp.*, 31(139):652–660, 1977.

[WRKH09] D. Walfish, J.K. Ryan, R.M. Kirby, and R. Haimes. One-sided smoothness-increasing accuracy-conserving filtering for enhanced streamline integration through discontinuous fields. *Journal of Scientific Computing*, 38:164–184, 2009.